AD-A057 651 ILLINOIS UNIV AT URBANA-CHAMPAIGN COORDINATED SCIENCE LAB F/G 9/5
A NEW METHOD FOR THE ANALYSIS OF DIELECTRIC WAVEGUIDES FOR MILL--ETC(U)
APR 78 P YANG DAAB07-72-C-0259
UNCLASSIFIED R-813 NL

| OF |

AD
A057 651

END
DATE
FILMED
9-78
DDC

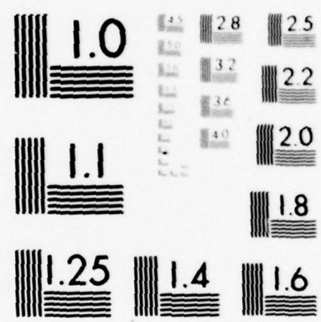

MICROCOPY RESOLUTION TEST CHART

NATIONAL BUREAU OF STANDARDS-1963-A

LEVEL II

12

REPORT R-813 MAY, 1978 UILU-ENG 78 2206

AD A057651

CSL COORDINATED SCIENCE LABORATORY

A NEW METHOD FOR THE ANALYSIS OF DIELECTRIC WAVEGUIDES FOR MILLIMETER WAVE AND OPTICAL INTEGRATED CIRCUITS

PING YANG

UNIVERSITY OF ILLINOIS - URBANA, ILLINOIS

UNCLASSIFIED

SECURITY CLASSIFICATION OF THIS PAGE (When Data Entered)

REPORT DOCUMENTATION PAGE		READ INSTRUCTIONS BEFORE COMPLETING FORM
1. REPORT NUMBER	2. GOVT ACCESSION NO.	3. RECIPIENT'S CATALOG NUMBER
4. TITLE (and Subtitle) A NEW METHOD FOR THE ANALYSIS OF DIELECTRIC WAVEGUIDES FOR MILLIMETER WAVE AND OPTICAL INTEGRATED CIRCUITS		5. TYPE OF REPORT & PERIOD COVERED Technical Report
		6. PERFORMING ORG. REPORT NUMBER R-813; UILU-ENG 2206
7. AUTHOR(s) Ping Yang		8. CONTRACT OR GRANT NUMBER(s) DAAB-07-72-C-0259
9. PERFORMING ORGANIZATION NAME AND ADDRESS Coordinated Science Laboratory University of Illinois at Urbana-Champaign Urbana, Illinois 61801		10. PROGRAM ELEMENT, PROJECT, TASK AREA & WORK UNIT NUMBERS
11. CONTROLLING OFFICE NAME AND ADDRESS Joint Services Electronics Program		12. REPORT DATE April, 1978
		13. NUMBER OF PAGES 71
14. MONITORING AGENCY NAME & ADDRESS(if different from Controlling Office)		15. SECURITY CLASS. (of this report) UNCLASSIFIED
		15a. DECLASSIFICATION/DOWNGRADING SCHEDULE

16. DISTRIBUTION STATEMENT (of this Report)

Approved for public release; distribution unlimited

17. DISTRIBUTION STATEMENT (of the abstract entered in Block 20, if different from Report)

18. SUPPLEMENTARY NOTES

19. KEY WORDS (Continue on reverse side if necessary and identify by block number)

Dielectric Waveguides
Millimeter Wave and Optical Integrated Circuits

20. ABSTRACT (Continue on reverse side if necessary and identify by block number)

A new method for the analysis of dielectric waveguides for millimeter and optical integrated circuits and a new dielectric waveguide structure are presented. A comparison between this new method and the previously available approaches by Itoh is given. Experimental results are described and the agreement between theory and experiment is shown to be quite good.

DD FORM 1 JAN 73 1473 EDITION OF 1 NOV 65 IS OBSOLETE

UNCLASSIFIED

SECURITY CLASSIFICATION OF THIS PAGE (When Data Entered)

ACCESSION for
NTIS White Section
DDC Buff Section
UNANNOUNCED
JUSTIFICATION

BY
DISTRIBUTION/AVAILABILITY CODES
Dist. AVAIL. and/or SPECIAL
A

LEVEL II

12

14 R-813, UILU-ENG-78-2206

9 Master's thesis,

6 A NEW METHOD FOR THE ANALYSIS OF DIELECTRIC WAVEGUIDES FOR MILLIMETER WAVE AND OPTICAL INTEGRATED CIRCUITS.

by

10 Ping Yang 11 Apr 78 12 78 p.

This work was supported in part by the Joint Services Electronics Program (U.S. Army, U.S. Navy and U.S. Air Force) under Contract DAAB-07-72-C-0259.

15 DAAB-07-72-C-0259

A NEW METHOD FOR THE ANALYSIS OF DIELECTRIC WAVEGUIDES FOR MILLIMETER WAVE AND OPTICAL INTEGRATED CIRCUITS

BY

PING YANG

B.S. National Taiwan University, 1974

THESIS

Submitted in partial fulfillment of the requirements
for the degree of Master of Science in Electrical Engineering
in the Graduate College of the
University of Illinois at Urbana-Champaign, 1978

Thesis Adviser: Professor Raj Mittra

Urbana, Illinois

ABSTRACT

A new method for the analysis of dielectric waveguides for millimeter and optical integrated circuits and a new dielectric waveguide structure are presented. A comparison between this new method and the previously available approaches by Itoh is given. Experimental results are described and the agreement between theory and experiment is shown to be quite good.

ACKNOWLEDGEMENT

The author wishes to express his sincere gratitude to Professor Raj Mittra and Dr. Ron Menendez, who contributed the original theoretical concept and provided assistance with the experiment.

TABLE OF CONTENTS

I. INTRODUCTION

Dielectric guiding structures for millimeter wave frequencies are low-loss, inexpensive, transmission media which can replace conventional metallic waveguides useful at lower frequencies.

Traditional metal waveguides, coaxial cables, and microstrip guides designed for transmission at microwave frequencies become increasingly lossy and expensive to manufacture for millimeter wave frequencies. With the advent of low-loss, high relative permittivity dielectric materials, dielectric guiding structures have received considerable attention for these applications. Dielectric waveguides offer the possibility reducing both losses and manufacturing expenses.

A primary source of loss in metallic guiding structures is Joule heating of the metallic surfaces. By confining the field with dielectric interfaces and away from conducting materials, this Joule loss can be largely eliminated. A second loss mechanism, scattering from surface irregularities, is directly related to the expense of conventional guides. In order to minimize scattering losses, conventional guides must be fabricated to precise tolerances. Dielectric guides that are typically larger dimensionally than their conventional counter parts, offer relaxed tolerance requirements on this fabrication.

By exploiting the dielectric guiding scheme to the fullest, monolithic integrated structures which place a complete transmitter or receiver circuit on a single dielectric slab are feasible.

Several components such as oscillators, mixers, phase shifters, directional couplers and antennas could be molded into a single sheet

of dielectric material. The ease of fabrication of dielectric materials by injection molding or stamping means such integrated circuits could be inexpensively produced.

As elaborated above, dielectric guides are an attractive candidate for further study. A great deal of work in this area has been contributed by McLevige, Itoh and Mittra,[1] Itoh,[2] Knox and Toulios,[3-8] Kloh, Armata, Jr. and Chrepta,[9] Chrepta and Jacobs,[10-11] Chang and Kuno,[12-13] Levin and Kietz,[14] Takano and Hamasaki,[15] Oxley, et. al.,[16] Schneider,[17] and Marcatilli.[18-19] Marcatilli, however analysis of these structures is difficult because one is forced to deal with non-separable geometries. An approximate solution which circumvents this difficulty, the effective dielectric constant (EDC) method, was introduced by Knox and Toulios[8] in 1970. This present work represents a generalization of the EDC method by recognizing the previously undiscussed role of polarization. The generalization may be termed an effective dielectric parameter method which is comprised of two complementary techniques: (1) the effective permitivity method which is equivalent to the EDC method and, (2) a novel approach, the effective permeability method. The central notion, discussed fully in Sections II A-E is to slice up the non-separable structure into two or more structures which are soluble by separation of variables.

After solving boundary value equations, each region can now be approximated by effective dielectric constants. Then the data in the revised problem can again be computed by separation of variables, the propagation constants k_z can now be determined.

The effective permeability method is a new method which is based on the same principle as the effective dielectric constant method, but instead

of using effective permitivity to approximate each region, it utilizes effective permeability. The theoretical reasons for the choice of using effective permitivity of effective permeability are discussed thoroughly in Section II-C.

A number of practical guiding structures are analyzed by this approach. Two forms of the inverted strip (IS) guide (Fig. 1A) introduced by McLevige, Itoh, and Mittra[1] and Itoh[2] are addressed: (1) a quartz-teflon (QT) guide composed of a quartz guiding layer resting on a teflon strip and (2) a homogeneous inverted strip (HIS) guide, so named because it is composed of single dielectric material. A new guide structure with many advantages, the homogeneous inverted strip (HIS) guide (Fig. 1b) is introduced in Section II-F, and the familiar rectangular dielectric rod guide (Fig. 1c) is also discussed.

In addition to the theoretical analysis, experimental verification of the predicted field configurations of the first three guides have been carried out as discussed in Section III.

From the data obtained in the research on homogeneous inverted strip waveguides (HIS) and quartz-teflon guide (QT), the experimental results of the dominant mode wavelength agree quite well with calculated results using effective permitivity method. Experimental results also show that there exists a second mode. The calculated second mode wavelength of QT guide using effective permitivity method also agrees closely with experimental results; but the calculated second mode wavelength of HIS guide doesn't agree with experimental results. Thus, the effective permeability method was devised to solve the waveguide problems in order to determine whether

the calculated results agree with the experimental results. It turned out to be the case. The comparison for the experimental results and both methods calculated results are shown from Table 1 to Table 13. Since both methods can only give approximate solutions to the problems, the experimental results are the only reliable data. Even so, we still want to be able to predict the results before devices are made and measurements are taken. Both methods are simple and they do provide good approximations. However, they are more believable if the calculated results of both methods agree with each other.

Finally, both methods are used for iteration. One method is used first, and the results are used as approximation fields for the other method, then the results are used as approximation fields for the first method. At first, there are differences between the two results but after a few iteration steps, all solutions converge to the same value.

The cross section of all these guides are given in Figure 1, the experimental results and calculated results are given from Table 1 to Table 13.

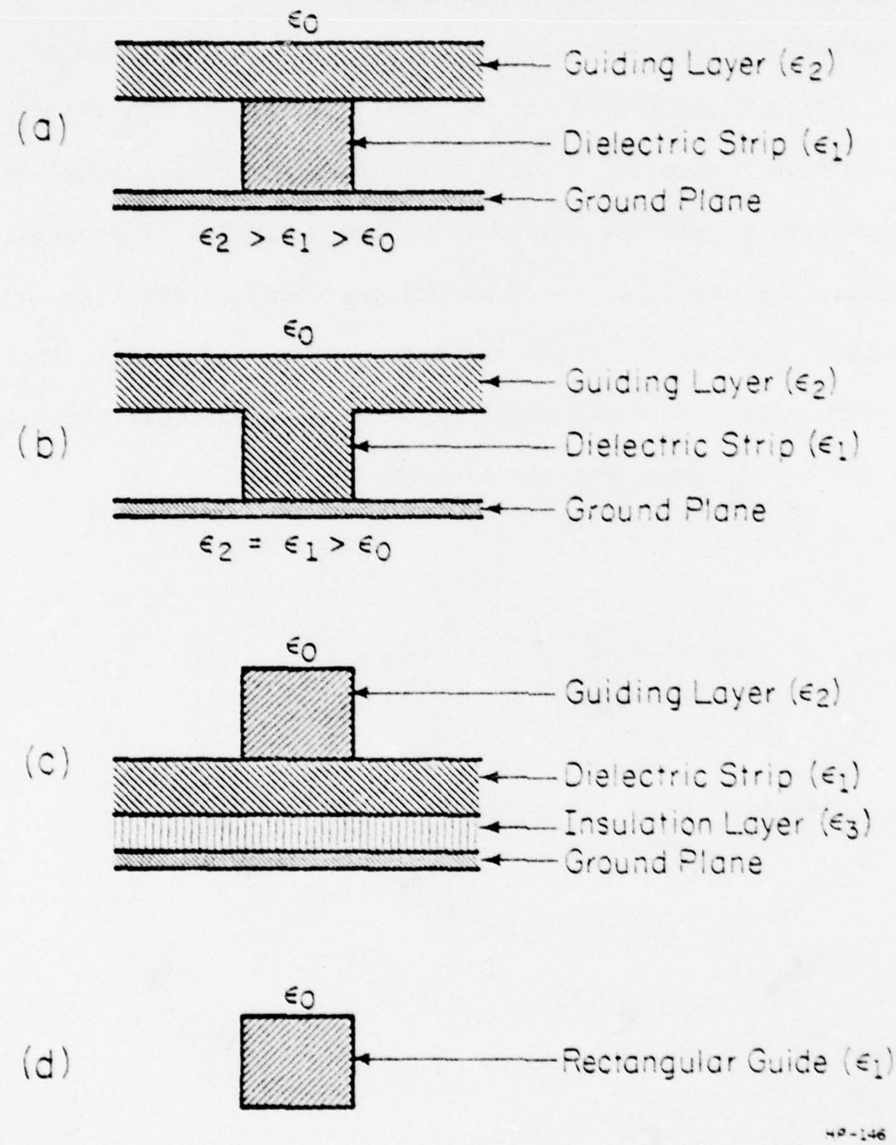

Figure 1. Cross sections of the dielectric waveguides analyzed in this paper: (a) inverted strip waveguide, (b) homogeneous inverted strip waveguide, (c) strip loaded insulated waveguide, (d) rectangular waveguide.

II. THEORETICAL ANALYSIS

A. Maxwell's Equations for TM_y MOde and TE_y Mode

The dielectric waveguides will generally support two types of modal fields. These modal fields can be classified as the E^y_{pq} and E^x_{pq} modes, where we have chosen the x and y directions to be horizontal and vertical, respectively, and the z-axis to be the direction of propagation.(Fig. 2) In the E^y_{pq} mode, the principal component of the electric field is aligned with the x-axis of the guide. These two modes are hybrid modes. It is possible to write fields of these modes in terms of two scalar potentials, ϕ^e and ϕ^h. One is TM_y mode, and the other is TE_y mode.

The field components are:[20]

$$E_y = 1/\varepsilon_r(y)\ (\partial^2/\partial y^2 + k^2)\ \phi^e \tag{1}$$

$$E_z = -jk_z/\varepsilon_r(y)\ \ \partial\phi^e/\partial y \tag{2}$$

E^y_{pq}

$$E_x = 1/\varepsilon_r(y)\ \partial^2\phi^e/\partial y\partial x \tag{3}$$

(TM_y)

$$H_y = 0 \tag{4}$$

$$H_z = j\omega\varepsilon_0\ \partial\phi^e/\partial x \tag{5}$$

$$H_x = -\omega\varepsilon_0\ k_z\ \phi^e \tag{6}$$

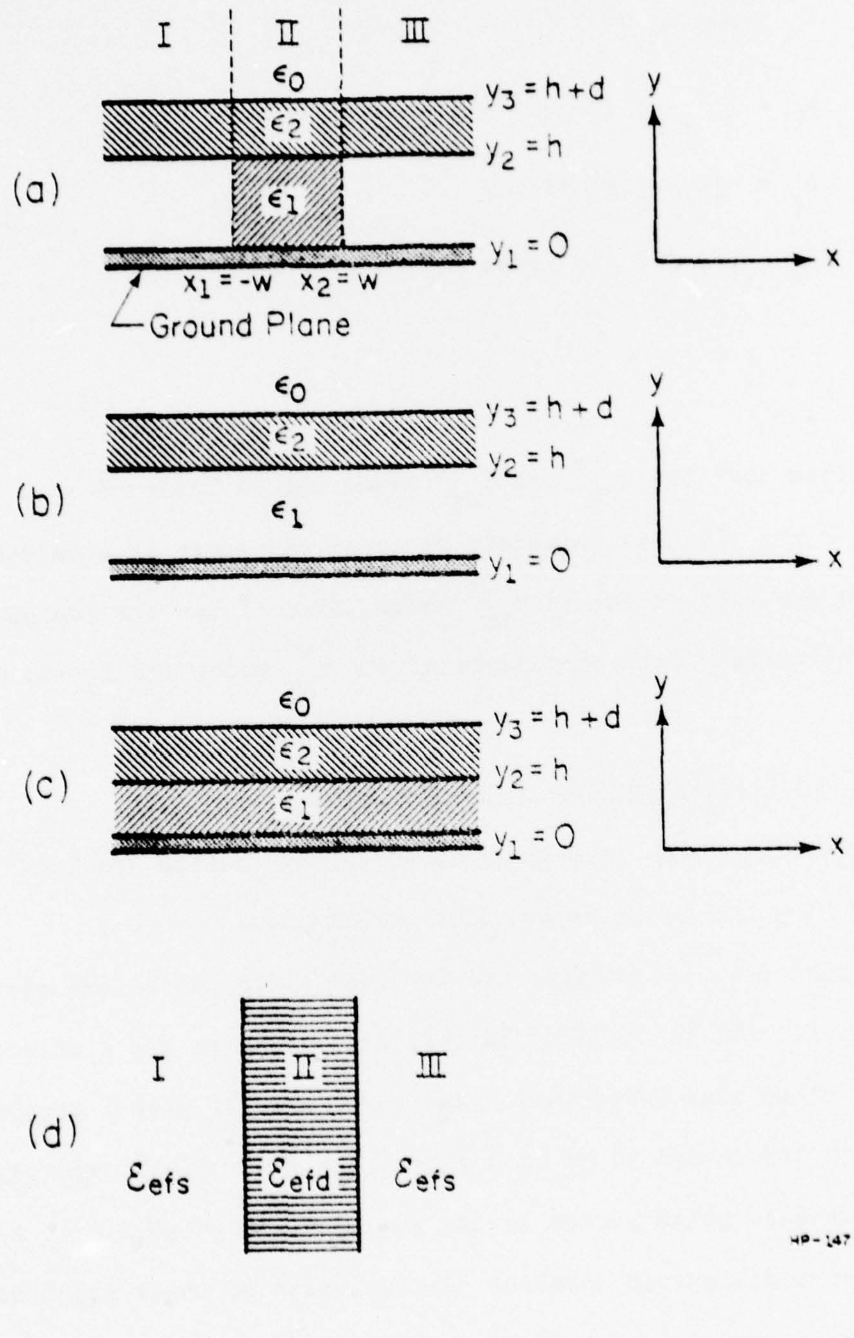

Figure 2. Analysis of inverted strip guide by means of effective dielectric constant method; (a) cross section, (b) single slab model for y-variation analysis, (c) double slab model for y-variation analysis, (d) model for x-variation analysis.

$$E_y = 0 \tag{7}$$

$$E_z = -j\omega\, \mu_0\, \partial\phi^h/\partial x \tag{8}$$

E^x_{pq}

$$E_x = \omega\mu_0\, k_z\, \phi^h \tag{9}$$

(TE_y)

$$H_y = 1/\mu_r(y)\ (\partial^2/\partial y^2 + k^2)\ \phi^h \tag{10}$$

$$H_z = -jk_z/\mu_r(y)\ \partial\phi^h/\partial y \tag{11}$$

$$H_x = 1/\mu_r(y)\ \partial^2\phi^h/\partial y\partial x \tag{12}$$

Since both the $E_{pq}^{\ y}$ and $E_{pq}^{\ x}$ modes can be analyzed in a similar manner, if the width to thickness ratio of the strip is moderately large, and if we try only to excite $E_{pq}^{\ y}$ modes, then ϕ^e has the dominant contribution and the principal field components of the E^y_{pq} modes are E_y and H_x.

B. <u>The Effective Dielectric Constants Method</u>

This method was originally developed by Toulios and Knox[8] and extended to the SDG and ISG by McLevige, Itoh and Mittra.[1,2]

Figure 2(a) illustrates the inverted strip guide, and each of the regions I, II, III is taken to be infinitely long in the x direction. Now there are three slab waveguides: regions I and III have a single-slab raised from the ground plane by a distance h (Fig. 2(b)), and region II is a double-slab guide backed by the ground plane (Fig. 2(c)). According to the effective dielectric constant concept, both of these structures can then be replaced by equivalent infinite homogeneous regions having effective dielectric ε_{efd} (for region II) and ε_{efs} (for region I and III).

where

$$\varepsilon_{efd} = \varepsilon_2 - k_{yd}^2/k_o^2 \tag{13}$$

$$\varepsilon_{efs} = \varepsilon_2 - k_{ys}^2/k_o^2 \tag{14}$$

After replacing Regions I, II, and III by the hypothetical medium with the effective dielectric constants ε_{efs} and ε_{efd}, respectively, the propagation constants k_z may be determined by matching the fields at each vertical interface of a three-layer structure as shown in Fig. 2(d).

The eigenvalue equation for k_z is obtained from:

$$k_z^2 = \varepsilon_{efd}\, k_o^2 - k_x^2 = \varepsilon_{efs}\, k_o^2 + \xi^2 \tag{15}$$

$$(\xi^2 - k_x^2) \sin [k_x (x_2-x_1)] + 2\xi\, k_x \cos [k_x(x_2-x_1)] = 0 \tag{16}$$

C. The Reasons for Using Effective Dielectric Constants

It has never been clearly explained why these structures are replaced by the effective dielectric constant (ε) rather than effective permeability (μ) when this method is used.

In the following, we will attempt to give an explanation, and then a new method for solving the same problem is introduced.

1. Consider a simple problem, a plane TE wave incident obliquely from medium I into medium II as shown in Fig. 3(a). The reflection coefficient is given by:

$$R = E_r/E_i = (\eta_2 \cos \theta_i - \eta_1 \cos \theta_t)/(\eta_2 \cos \theta_i + \eta_1 \cos \theta_t) \tag{17}$$

where $\eta_2 = \sqrt{\mu_2/\varepsilon_2}\ \eta_o \quad \eta_1 = \sqrt{\mu_1/\varepsilon_1}\ \eta_o \quad \eta_o = \sqrt{\mu_o/\varepsilon_o}$ (18)

Now if region I is replaced by an effective dielectric constant ε_1^*

$$\varepsilon_1^* = \varepsilon_1 - K_{y1}^2/\mu_1 k_o^2 \tag{19}$$

replace region II by an effective dielectric constant ε_2^*.

$$\varepsilon_2 = \varepsilon_2^* - K_{y2}^2/\mu_2 k_o^2 \tag{20}$$

and then assume the plane TE wave incidents normally to the interface as shown in Fig. 3(b).

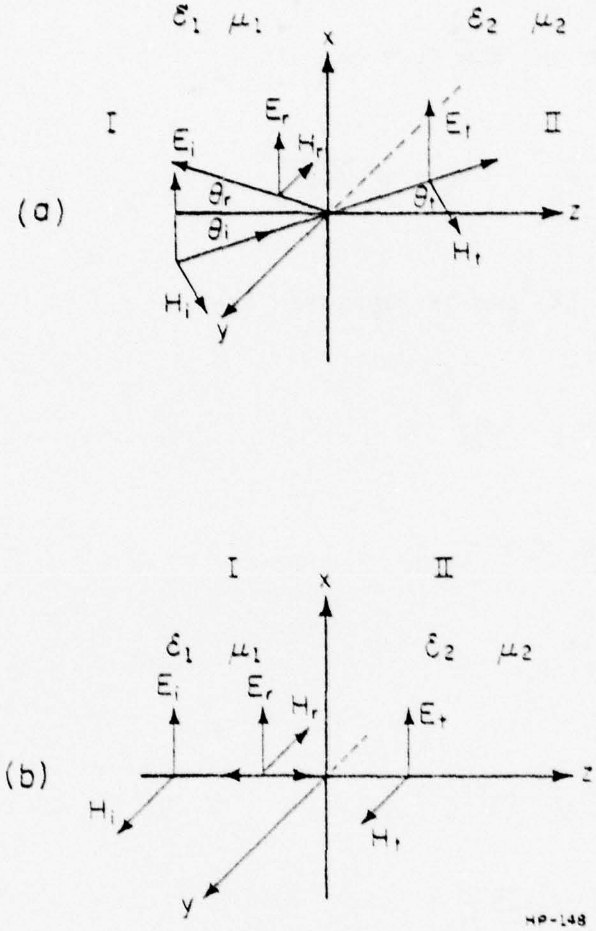

Figure 3. (a) Plane TE-wave incidents obliquely from medium I to medium II.
(b) Equivalent problem of (a).

Because the incident angle θ_i and the transmission angle, θ_t must obey Snell's law, namely:

$$k_{y1} = k_{y2} = -k_1 \sin \theta_i = -k_2 \sin \theta_t \tag{21}$$

where $k_1 = k_o \sqrt{u_1 \varepsilon_1} \qquad k_2 = k_o \sqrt{u_2 \varepsilon_2}$ (22)

Equations (7) and (8) can be rewritten as:

$$\varepsilon_1^* = \varepsilon_1 - k_{y1}{}^2/u_1 k_o{}^2 \tag{19}$$

$$= \varepsilon_1 - \varepsilon_1 \sin^2 \theta_i$$

$$= \varepsilon_1 \cos^2 \theta_i \tag{23}$$

$$\varepsilon_2^* = \varepsilon_2 - k_{y2}{}^2/u_2 k_o{}^2 \tag{20}$$

$$= \varepsilon_2 - \varepsilon_2 \sin^2 \theta_t$$

$$= \varepsilon_2 \cos^2 \theta_t \tag{24}$$

The reflection coefficient R^* for this new problem is:

$$R^* = (\sqrt{\varepsilon_1^*/\mu_1} - \sqrt{\varepsilon_2^*/\mu_2}) / (\sqrt{\varepsilon_1^*/\mu_1} + \sqrt{\varepsilon_2^*/\mu_2}) \qquad (25)$$

After substituting equations (23) and (24) into (25), we obtain

$$R^* = (1/n_1 \cos \theta_i - 1/n_2 \cos \theta_t)/(1/n_1 \cos \theta_i + 1/n_2 \cos \theta t)$$

$$= (n_2 \cos\theta_i - n_1 \cos\theta t) / (n_2 \cos \theta_i + n_1 \cos \theta t)$$

$$= R.$$

It is possible to show that if region I and II are replaced by the effective permeability, the same reflection coefficient cannot be obtained.

2. Secondly, if a plane TM wave incidents obliquely from medium I into medium II as in Fig. 4(a), the reflection coefficient

$R = H_r/H_i = E_r/E_i$ is

$$R = (n_2 \cos \theta t - n_1 \cos \theta_i) / (n_1 \cos \theta_i + n_2 \cos \theta_t) \qquad (27)$$

Now if region I is replaced by an effective permeability μ_1^*

(a)

(b)

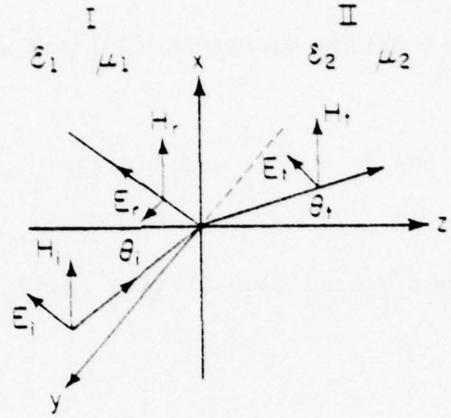

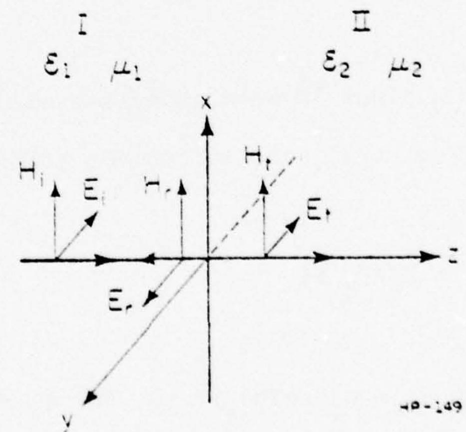

Figure 4. (a) Plane TM-wave incidents obliquely from medium I to medium II.
(b) Equivalent problem of (a).

$$\mu_1^* = \mu_1 - k_{y1}^2/\varepsilon_1 k_o^2 \tag{28}$$

$$= \mu_1 - \mu_1 \sin^2 \theta_i$$

$$= \mu_1 \cos^2 \theta_i \tag{29}$$

and if Region II is replaced by an effective permeability μ_2^*,

$$\mu_2{}^* = \mu_2 - k_{y2}^2/\varepsilon_2 k_o{}^2 \tag{30}$$

$$= \mu_2 - \mu_2 \sin^2 \theta_t$$

$$= \mu_2 \cos^2 \theta_t \tag{31}$$

and, finally, if it is assumed that the plane TM-wave incidents normally to the interface as shown in Fig. 4(b), the reflection coefficient R* for this new problem is

$$R^* = (\sqrt{\mu_2{}^*/\varepsilon_2} - \sqrt{\mu_1{}^*/\varepsilon_1}) / (\sqrt{\mu_2{}^*/\varepsilon_2} + \sqrt{\mu_1^*/\varepsilon_1}) \tag{32}$$

After substituting equations (29) and (31) into (32), we obtain

$$R^* = (n_2 \cos \theta_t - n_1 \cos \theta_i)/(n_1 \cos \theta_i + n_2 \cos \theta_t) = R \tag{33}$$

Similarly, if Region I and II are replaced by effective dielectric constants, the same reflection coefficient cannot be obtained.

3. In short, the polarization of the plane wave determines whether effective ε or effective μ should be used. For TE wave, effective ε must be used. For TM wave, effective μ must be used.

4. The eigenvalue equations for the slab guide can now be derived by using the above concept. If it is TE wave as shown in Fig. 5(a):

$$k_{x1}^2 + k_{z1}^2 = \mu_1 \varepsilon_1 k_o^2 \tag{34}$$

$$k_{x2}^2 + k_{z2}^2 = \mu_2 \varepsilon_2 k_o^2 \tag{35}$$

$$k_{z1} = k_{z2} \tag{36}$$

the effective dielectric constants are:

$$\varepsilon_1{}^* = \varepsilon_1 - k_{z1}^2/\mu_1 k_o^2 \tag{37}$$

$$= k_{x1}^2/\mu_1 k_o^2 \tag{38}$$

$$\varepsilon_2{}^* = \varepsilon_2 - k_{x2}^2/\mu_2 k_o^2 \tag{40}$$

$$= k_{x2}^2/\mu_2 k_o^2$$

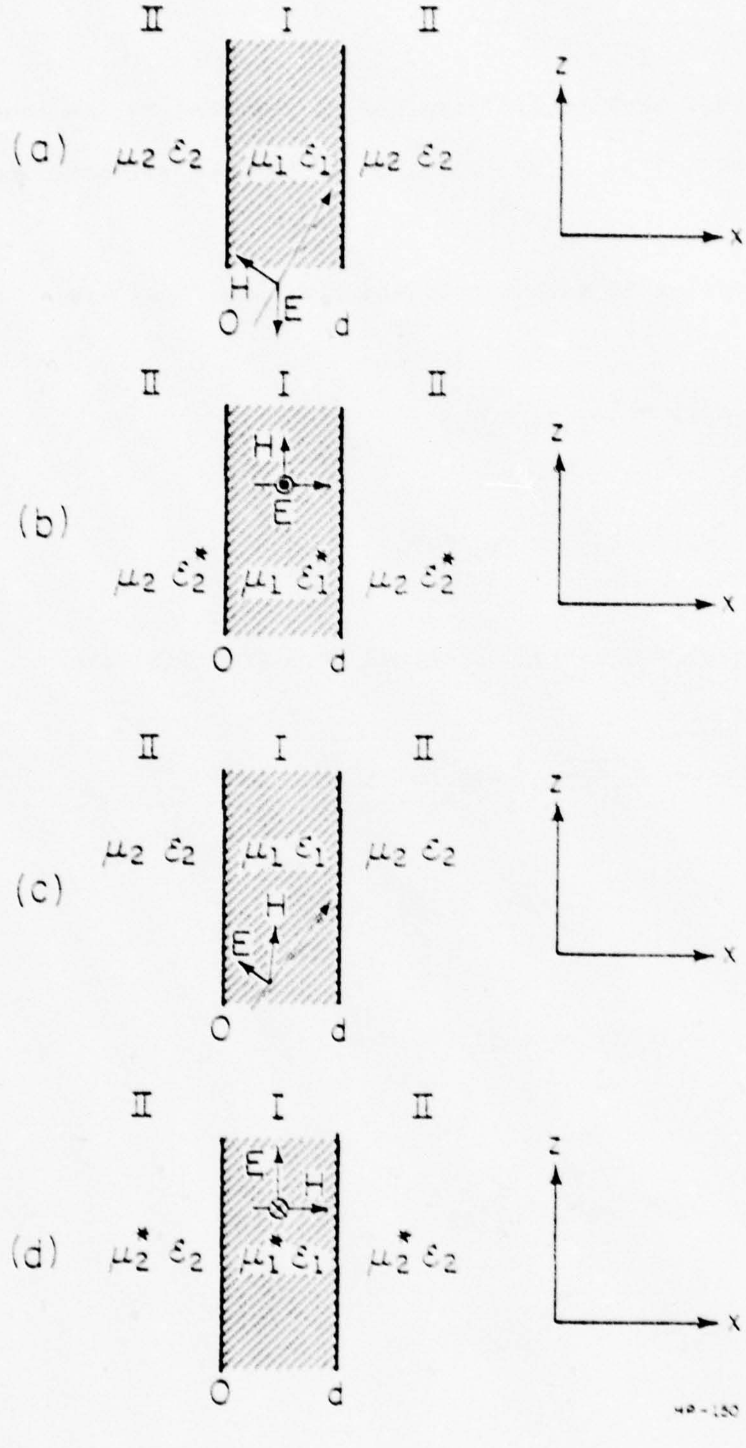

Figure 5. (a) TE-wave inside a slab guide.
(b) Equivalent problem for (a).
(c) TM-wave inside a slab guide.
(d) Equivalent problem for (c).

The original problem 5(a) can now be replaced by the equivalent problem as shown in Fig. 5(b), in which a TEM wave resonates inside a slab guide.

The eigenvalue equations obtained from Fig. 5(a) are:

$$\text{sum } H_z \quad \tan(k_{x1}d/2) = j\mu_2 k_{x1}/\mu_1 k_{x2} \tag{41}$$

$$\text{antisym } H_z \quad \tan(k_{x1}d/2) = j\mu_1 k_{x2}/\mu_2 k_{x1} \tag{42}$$

The eigenvalue equations obtained from Fig. 5(b) are:

$$\text{sym } H_z \quad \sqrt{\mu_2/\varepsilon_2^*} = -j\sqrt{\mu_1/\varepsilon_1^*}\ \tan(k_{x1}d/2) \tag{43}$$

$$\text{antisym } H_z \quad \sqrt{\mu_2/\varepsilon_2^*} = j\sqrt{\mu_1/\varepsilon_1^*}\ \cot(k_{x1}d/2) \tag{44}$$

Equations (43), (44) can be simplified as:

$$\text{sym } H_z \quad \tan(k_{x1}d/2) = j\mu_2 k_{x1}/\mu_1 k_{x2} \tag{45}$$

$$\text{antisym } H_z \quad \tan(k_{x1}d/2) = j\mu_1 k_{x2}/\mu_2 k_{x1} \tag{46}$$

These are identical equations to equations (41) and (42). Therefore, we can get transverse eigenvalue equations for TE waves by the effective ε method.

5. If it is a TM wave as shown in Fig. 5(c), then:

$$k_{x1}^2 + k_{z1}^2 = \mu_1 \varepsilon_1 k_o^2 \quad (34)$$

$$k_{x2}^2 + k_{z2}^2 = \mu_2 \varepsilon_2 k_o^2 \quad (35)$$

$$k_{z1} = k_{z2} \quad (36)$$

and the effective permeabilities (μ's) are:

$$\mu_1^* = \mu_1 - k_{z1}^2/\varepsilon_1 k_o^2 \quad (47)$$

$$= k_{x1}^2/\varepsilon_1 k_0^2 \quad (48)$$

$$\mu_2^* = \mu_2 - k_{z2}^2/\varepsilon_2 k_o^2 \quad (49)$$

$$= k_{x2}^2/\varepsilon_2 k_o^2 \quad (50)$$

The original problem 5(c) can now be replaced by the equivalent problem as shown in Fig. 5(d), in which a TEM wave resonates inside a slab guide.

The eigenvalue equations obtained from Fig. 5(c) are:

$$\text{antisym } E_z \quad \tan\left(\frac{k_{x1} d}{2}\right) = j\,\frac{\varepsilon_1 k_{x2}}{\varepsilon_2 k_{x1}} \tag{51}$$

$$\text{sym } E_z \quad \tan\left(\frac{k_{x1} d}{2}\right) = j\,\frac{\varepsilon_2 k_{x1}}{\varepsilon_1 k_{x2}} \tag{52}$$

The eigenvalue equations obtained from Fig. 5(d) are:

$$\text{antisym } E_z \quad \sqrt{\frac{\mu_2^*}{\varepsilon_2}} = -j\,\sqrt{\frac{\mu_1^*}{\varepsilon_1}}\,\tan\left(\frac{k_{x1}}{2}\right) \tag{53}$$

$$\text{sym } E_z \quad \sqrt{\frac{\mu_2^*}{\varepsilon_2}} = j\,\sqrt{\frac{\mu_1^*}{\varepsilon_1}}\,\cot\left(\frac{k_{x1} d}{2}\right) \tag{54}$$

Rewrite (53) and (54) as:

$$\text{antisym } E_z \quad \tan\left(\frac{k_{x1} d}{2}\right) = j\,\frac{\varepsilon_1 k_{x2}}{\varepsilon_2 k_{x1}} \tag{55}$$

$$\text{sym } E_z \quad \tan\left(\frac{k_{x1} d}{2}\right) = j\,\frac{\varepsilon_2 k_{x1}}{\varepsilon_1 k_{x2}} \tag{56}$$

These equations are identical to (51) (52) and consequently, we can get transverse eigenvalue equations by the effective μ method for TM wave.

6. After determining the criterion for using effective ε or effective μ, let us consider again the inverted strip guide as shown in Fig. 6(a). The principal field components are E_y and H_x. From equations (2), (3), (5), we can see that E_x is a product of two small terms (so it is negligibly small). E_z and H_z are products of one small term with a large term (so they are minor components).

The field components are E_y, E_z, H_x, H_z as shown in Fig. 5(b), when each region is replaced by a hypothetical medium, for the interface YZ plane. It is a TE wave, therefore, we must use effective dielectric constant.

If we slice the Inverted Strip Guide in a different way as shown in Fig. 6(c), when each region is replaced by a hypothetical medium, the interface is XZ plane, it is a TM wave. Therefore, we must use effective permeability.

D. The Effective Permeability Method

Now the effective permeability method will be used to analyze the Inverted Strip Guide (ISG). In Figure 7(a) the Inverted Strip Guide is redrawn and each of the regions I, II, and III is taken to be infinitely

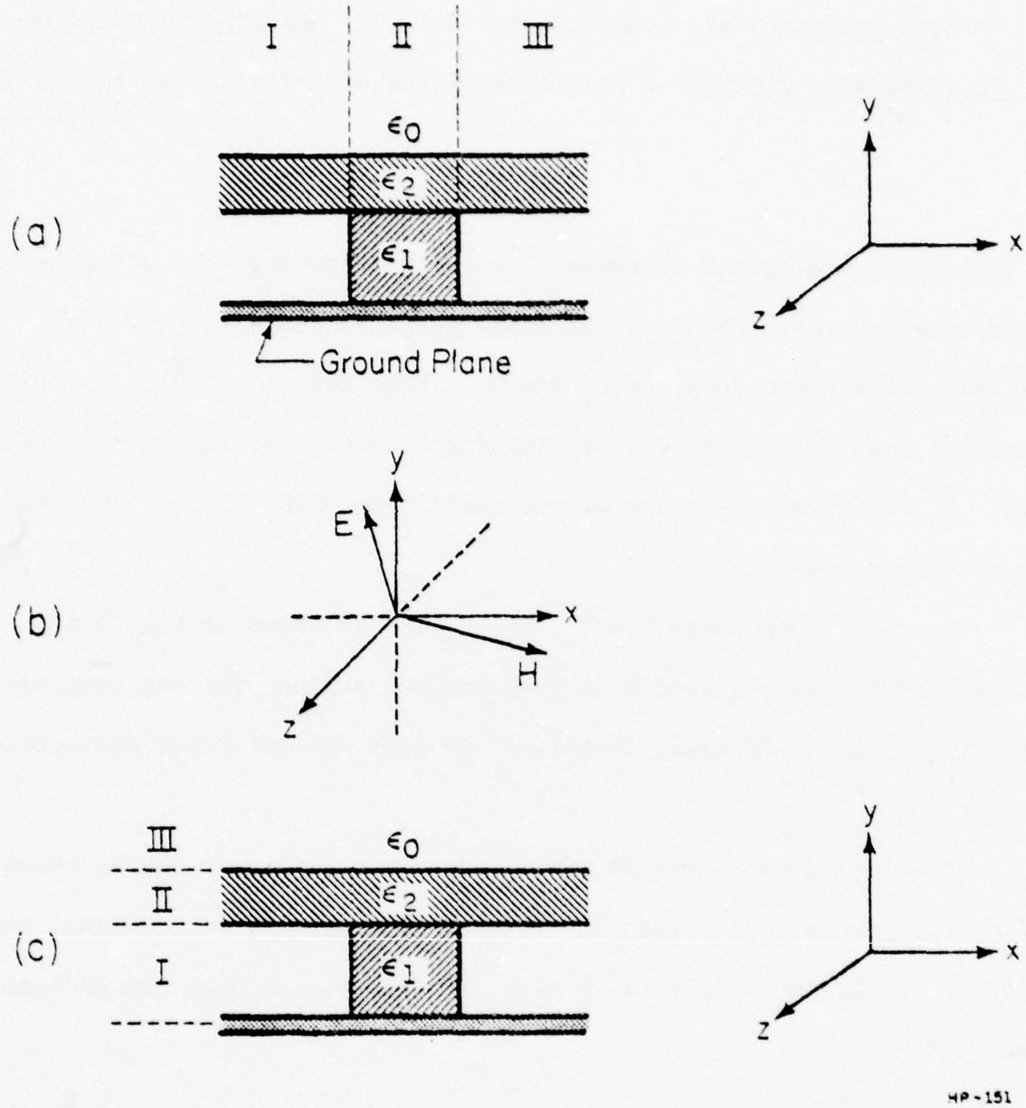

Figure 6. (a) Cross section of inverted strip guide sliced in the y-direction,
(b) all the field components
(c) Cross section of inverted strip guide sliced in the x-direction.

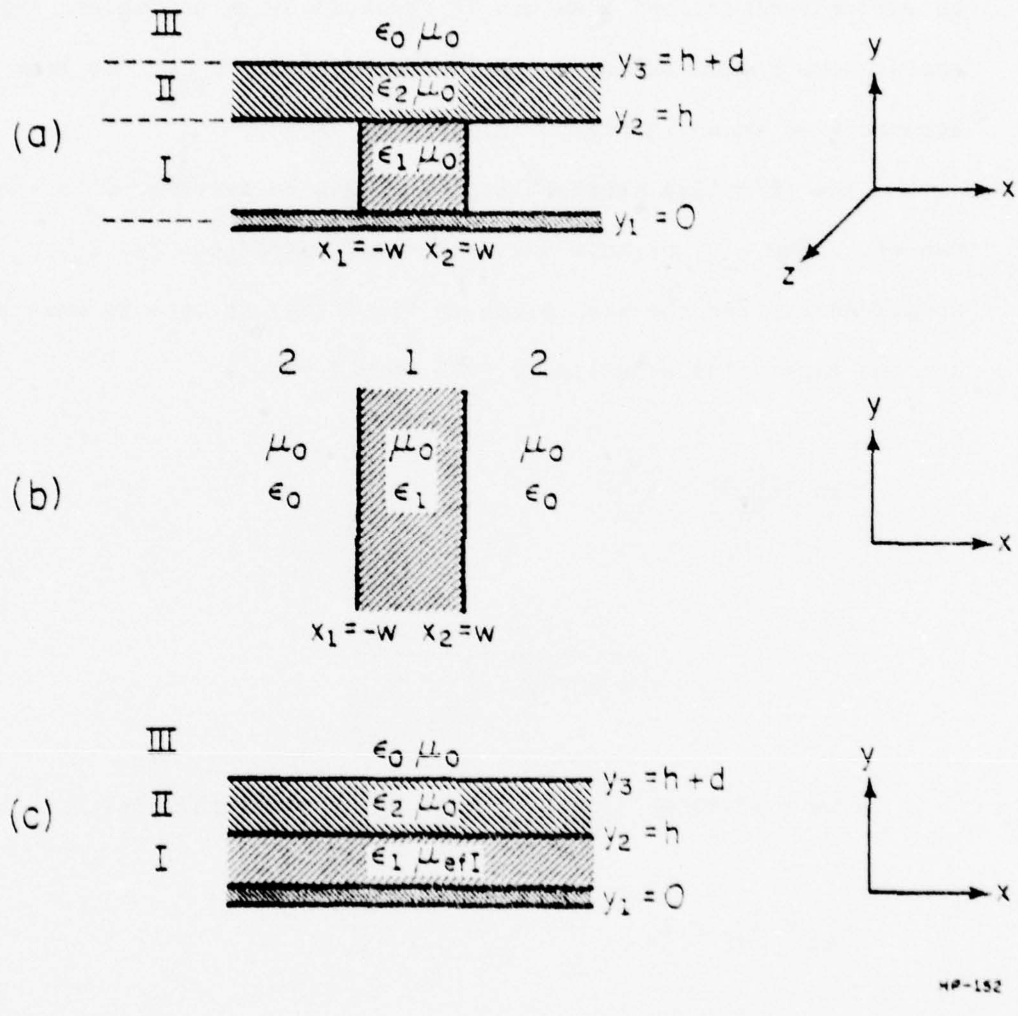

Figure 7. Analysis of inverted strip guide by means of effective permeability method, (a) cross section, (b) single slab model for x-variation analysis, (c) model for y-variation analysis

long in the y-direction. Regions II and III are now homogeneous regions. Region I is a single slab guide (Fig. 7 (b)). The propagation constant can be determined by matching the tangential electric and magnetic fields at each interface, and then can be replaced by an equivalent infinite homogeneous region having effective permeability μ_{ef1}. We then have a structure as shown in Fig. 7 (c).

The effective permeability μ_{ef1} may be determined in the following manner. From c(6) we know that the field components are E_y, E_z, H_x, H_z. Consequently, for the slab guide in Fig 7 (b), it is a TE wave problem, and the eigenvalue equation is (42) where d = 2w.

$$\tan (k_{x1} w) = \frac{jk_{x2}}{k_{x1}} \tag{42}$$

$$= \sqrt{(\varepsilon_1 - 1)k_0^2 - k_{x1}^2} \; / \; k_{x1} \tag{57}$$

The quantities k_{x1}, k_{z1}, k_{z2}, k_{x2} are related via:

$$k_{z1} = k_{z2} = k_z' \tag{58}$$

$$k_{x1}^2 + k_z'^2 = \varepsilon_1 k_0^2 \tag{59}$$

$$k_{x2}^2 + k_z'^2 = k_0^2 \tag{60}$$

The effective permeability for this structure is:

$$\mu_{ef1} = \mu_0 - \frac{k_{x1}^2}{\varepsilon_1 k_0^2} \tag{61}$$

We may now determine the propagation constant for structure 7(c) by matching the tangential fields at each interface. In the $(\varepsilon_1, \mu_{ef1})$ region, we allow for the possibility of the field being either sinusoidal or exponentially decaying by expressing it in terms of a sum of hyperbolic functions. The fields in the (ε_2, μ_0) region are sinusoidal and the fields in the (ε_0, μ_0) region are exponentially decaying.

The fields are the following:

$$\phi^e(y) = A \cosh(n_1 y) \qquad 0<y<h \tag{62}$$

$$\phi^e(y) = B_c \cos [K_y(y-h)] + B_s \sin [k_y(y-h)] \qquad h<y<h+d \tag{63}$$

$$\phi^e(y) = Ce^{-n_3(y-h-d)} \qquad y>h+d \tag{64}$$

where n_1 and n_3 are attentuation constants in their respective regions and subject to a relation of equation (65).

$$k_z^2 = k_0^2 + n_3^2 = \varepsilon_1 \mu_{ef1} k_0^2 + n_1^2 = \varepsilon_2 k_0^2 - k_y^2 \tag{65}$$

where n_3 must be real and positive, while n_1 may be either real or imaginary.

Matching the field components H_x and E_z at $y=h$, we obtain

$$A \cosh(n_1 h) = B_c \tag{66}$$

$$\frac{A\, n_1 \sinh(n_1 h)}{\varepsilon_1} = \frac{B_s k_y}{\varepsilon_2} \tag{67}$$

and similarly at $y = h + d$

$$B_c \cos[k_y d] + B_s \sin[K_y d] = C \tag{68}$$

$$\frac{-B_c k_y \sin(k_y d) + B_s K_y \cos(K_y d)}{\varepsilon_2} = -n_3\, C \tag{69}$$

After algebraically manipulating the four equations (66) through (69), we obtain:

$$B_c = A \cosh(n_1 h) \tag{70}$$

$$B_s = A \frac{\varepsilon_2 n_1}{\varepsilon_1 k_y} \sinh(n_1 h) \tag{71}$$

$$C = A \left[\cosh(n_1 h) \cos(k_y d) + \frac{n_1 \varepsilon_2}{\varepsilon_1 k_y} \sinh(n_1 h) \sin(k_y d)\right] \tag{72}$$

and the eigenvalue equation:

$$n_3\varepsilon_2\varepsilon_1 k_y \cosh(n_1 h)\cos(k_y d) + n_3\varepsilon_2^2\, n_1 \sinh(n_1 h)$$

$$\sin(k_y d) - \varepsilon_1 k_y^2 \cosh(n_1 h)\sin(k_y d) + k_y\varepsilon_2 n_1 \sinh(n_1 h)$$

$$\cos(k_y d) = 0 \tag{73}$$

After using a computer to solve (73) for k_y, we can then use equation (65) to calculate k_z.

E. Iteration Procedure

The Inverted Strip Guide can be divided into nine regions as shown in Fig. 8(a). From the effective dielectric constant method, we can obtain a set of k_x's and k_y's as shown in Fig. 8(b), where:

$$k_{x1}^{\varepsilon} = k_{x2}^{\varepsilon} = k_{x3}^{\varepsilon} \tag{74}$$

$$k_{x4}^{\varepsilon} = k_{x5}^{\varepsilon} = k_{x6}^{\varepsilon} \tag{75}$$

$$k_{x7}^{\varepsilon} = k_{x8}^{\varepsilon} = k_{x9}^{\varepsilon} \tag{76}$$

From the effective permeability method, we can obtain a set of k_x's and k_y's as shown in Fig. 8(c), where:

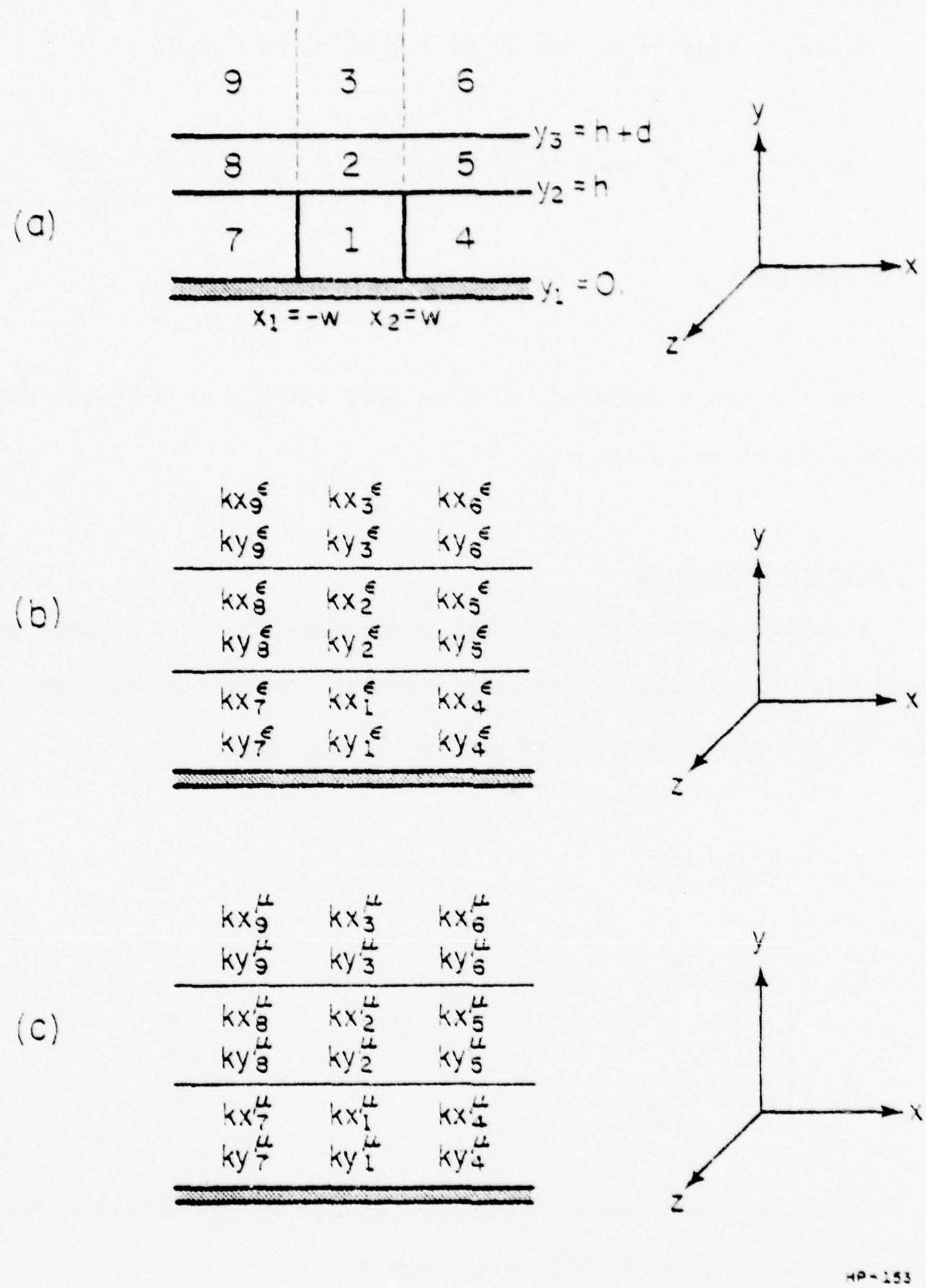

Figure 8. (a) Nine regions for inverted strip guide.
(b) k_x's and k_y'x obtained from effective ϵ method.
(c) k_x's and k_y's obtained from effective μ method.

$$k^{\mu}_{y1} = k^{\mu}_{y4} = k^{\mu}_{y7} \tag{77}$$

$$k^{\mu}_{y2} = k^{\mu}_{y5} = k^{\mu}_{y8} \tag{78}$$

$$k^{\mu}_{y3} = k^{\mu}_{y6} - k^{\mu}_{y9} \tag{79}$$

Equations (74) through (79) show the defects of the above two methods, since the true values of k_{x1}, k_{x2}, k_{x3} may not be the same, and etc.

If the true values of k_x's and k_y's lie between these two sets and these two sets of k_x's and k_y's are good approximations to the true set, then we may iterate and get a set of convergent values.

The iteration procedure is summarized below. First, use the effective ε method to find all the k^{ε}_x's and k^{ε}_y's. Then use the effective μ method to find all the k^{μ}_x's and k^{μ}_y's. And then average these two sets. There are many ways to average, such as arithmetic mean, geometric mean, root mean square, etc. The root mean square turns out to be the best way. It makes the set of values converge faster than any other method. It also preserves the value of k_z. Accordingly, we get a set of average k_x's and k_y's.

$$k_{x1\ av} = \sqrt{{k^{\varepsilon}_{x1}}^2 + {k^{\mu}_{x1}}^2} \tag{80}$$

$$k_{x2\ av} = \sqrt{{k^{\varepsilon}_{x2}}^2 + {k^{\mu}_{x2}}^2} \tag{81}$$

$$k_{x3\ av} = \sqrt{k_{x3}^{\varepsilon^2} + k_{x3}^{\mu^2}} \qquad (82)$$

" "

etc.

We then assume these average k_x's and k_y's are good approximations of the true values, and we use the effective ε method again. Taking into account the effect of the average k_x's to get effective μ's for each region, we then obtain a new set of k_x^ε's and k_y^ε's, and we use the effective μ method again with the effect of the average k_y's, (specifically, eliminating the effect of average k_y's by replacing each region by the effective μ). We then get a new set of k_x^μ's and k_y^μ's, average these two sets, use the effective ε method again, and use the effective μ method again. After a few steps, the values of these two sets will converge.

F. Strip-Loaded Insulated Guide

For the strip guide, (Fig. 9(a)) because most of the energy is in the guiding layer, so, the conductor loss is quite large. If we put a layer of low dielectric constant between the guiding layer and the ground plane as shown in Fig. 9(b), (because the fields are exponentially decaying in the insulation layer), the conductor loss is smaller. Furthermore, because the effective dimension of the guide is smaller, its propagation characteristics becomes mere single-moded. This point can be explained by

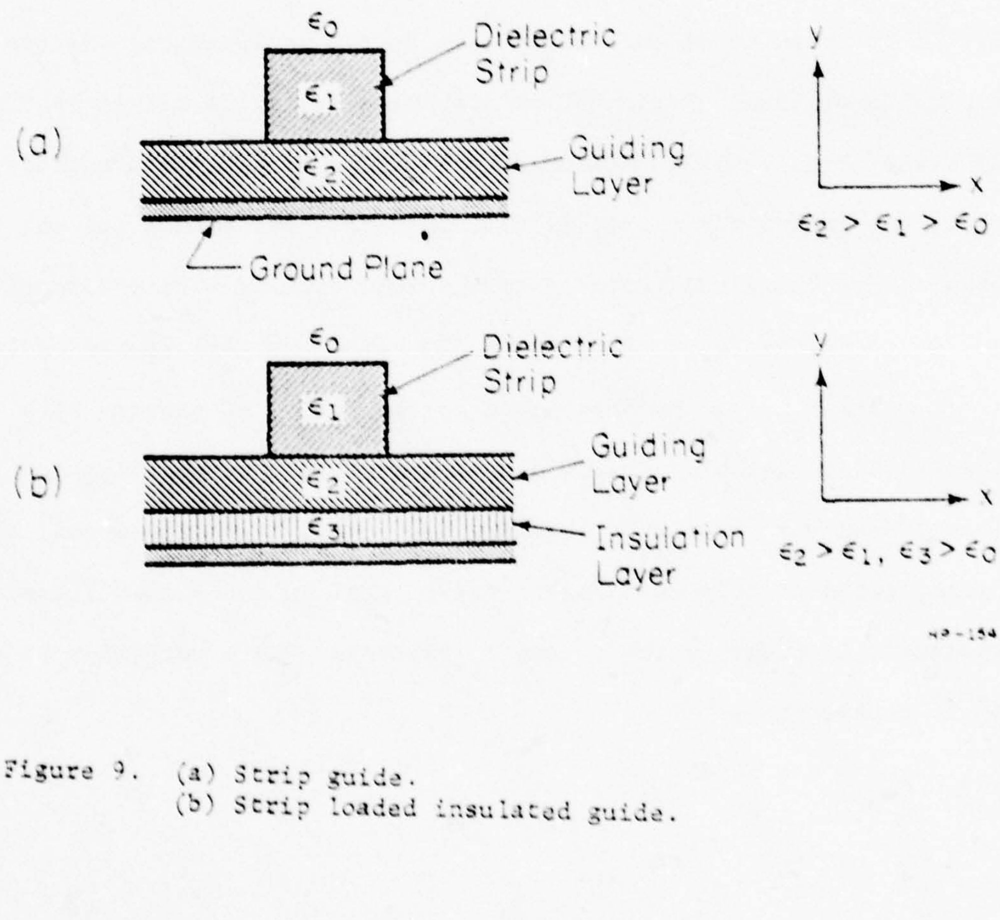

Figure 9. (a) Strip guide.
(b) Strip loaded insulated guide.

the following example. Suppose we now add a thin layer of air gap between the slab guide and the ground plane as shown in Fig. 10(a). If such a layer is added, then the y-variation of $|E_y|$ will be as shown in Fig. 10(b), and the k_y value will be 1222.05 1/m. If this air gap is not added, the y-variation of $|E_y|$ will be as shown in Fig 10(c), and the k_y value will be 751.51 1/m. Therefore, the effective dimension of the slab guide with an air gap is significantly smaller, even if the air gap is very thin.

Similarly, we have two simple methods to analyze this guide:

1) The Effective Dielectric Constants Method: In Figure 11(a), I have redrawn the strip-loaded insulated guide and each of the regions I, II, III is taken to be infinitely long in the x-direction. We now have three slab waveguides. Region II is a triple-slab guide backed by the ground plane (Fig. 11(b)). Regions I and III are double-slab guides backed by the ground plane (Fig 11(c)), both of these structures can then be replaced by equivalent infinite homogeneous regions having effective dielectric constants ε_{eft} (for Region II) and ε_{efd} (for Regions I and III).

ε_{eft} and ε_{efd} can be determined in the following manner. The double-slab model analysis is the same as previously noted. The triple slab model analysis is done by assuming the fields to be sinusoidal in the ε_2 region, exponentially decaying in the ε_0 region, and either sinusoidal or exponentially decaying the ε_3 and ε_1 regions. The y variation in the fields is thus written:

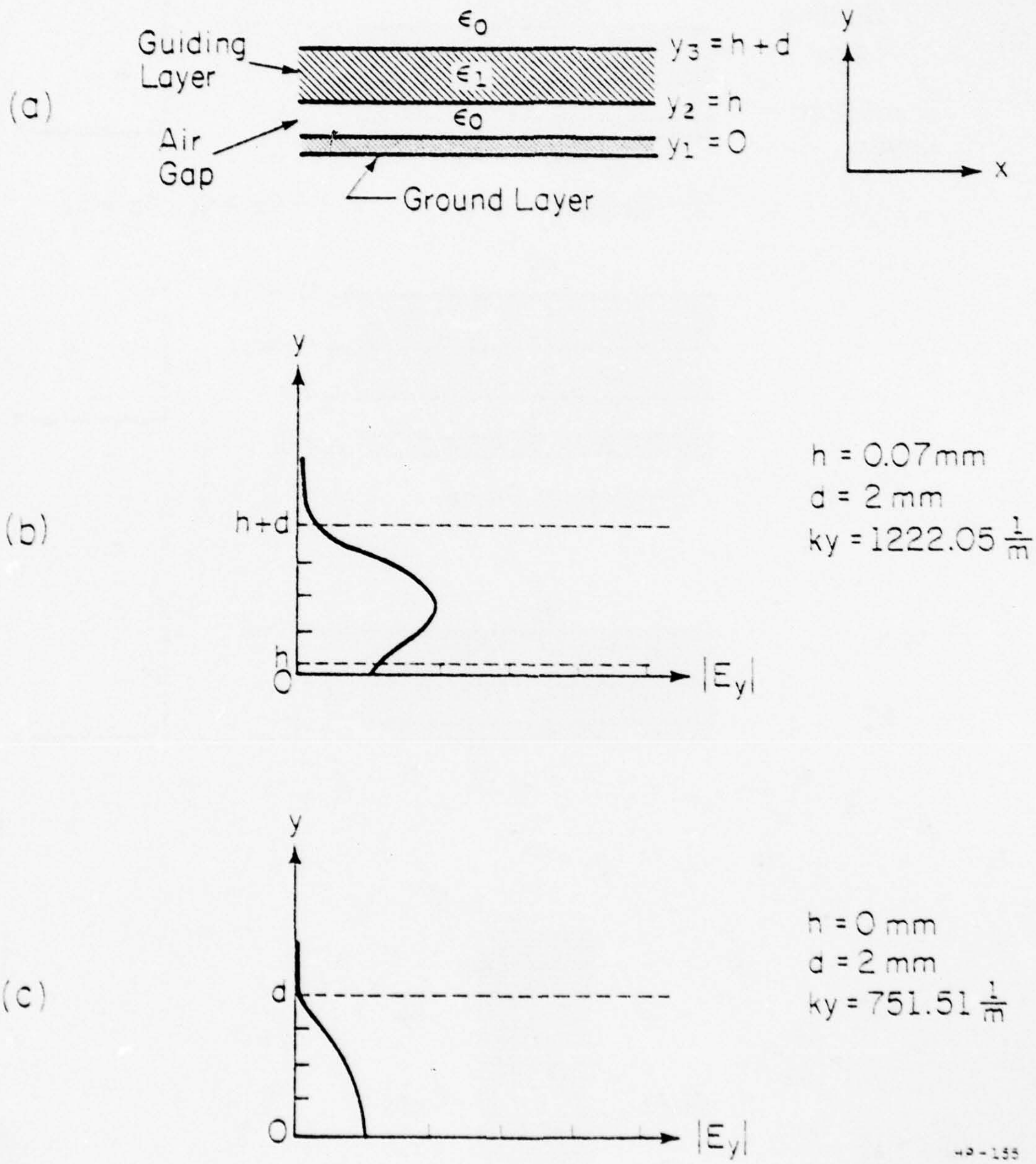

Frequency = 79 GHz

Figure 10. (a) Slab guide with a thin air gap between the guiding layer and the ground plane.
(b) y-variation of $|E_y|$ for (a).
(c) y-variation of $|E_y|$ for strip guide without air gap.

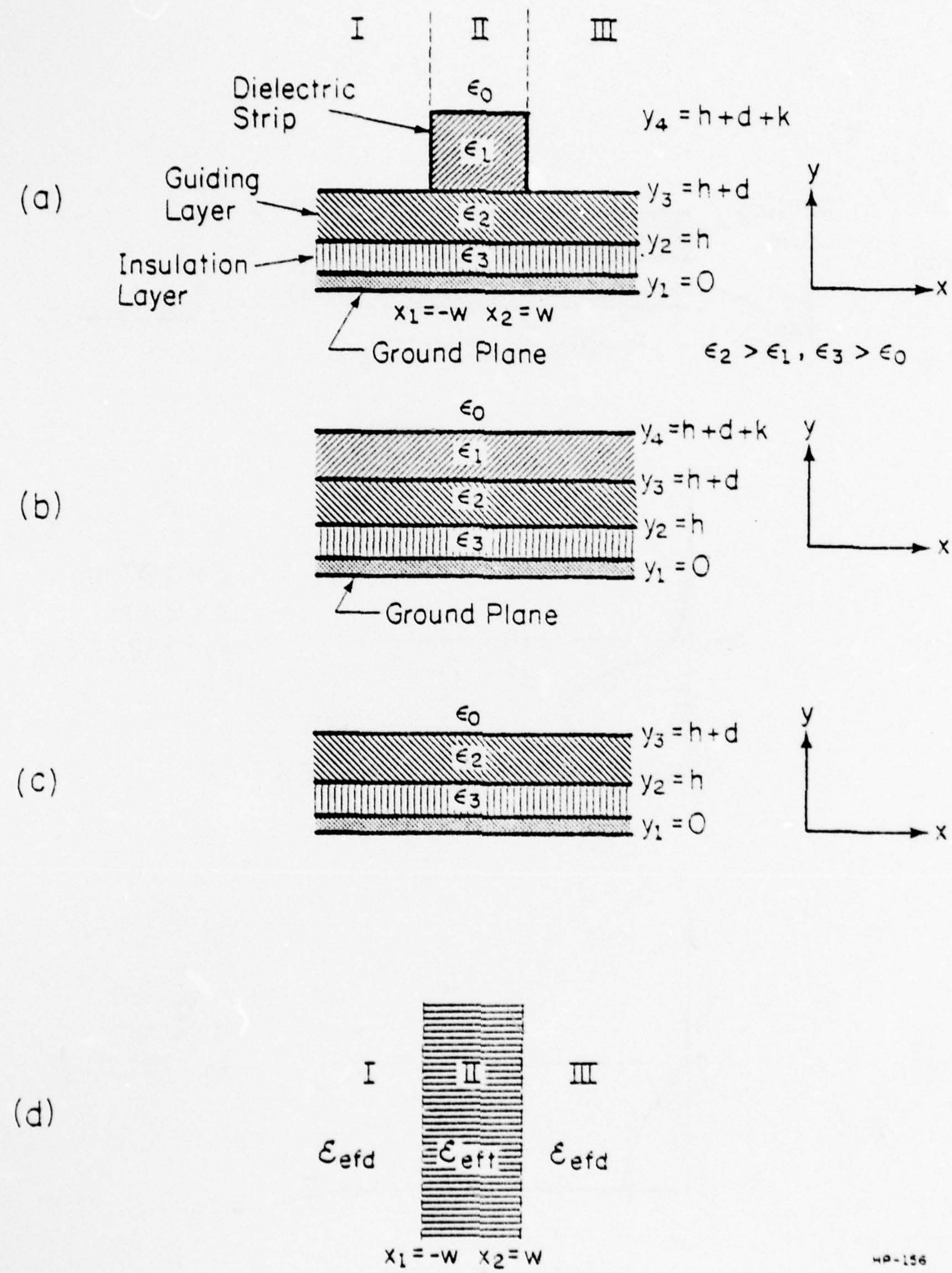

Figure 11. Analysis of strip loaded insulated guide by means of effective dielectric constant method: (a) cross section, (b) triple-slab model for y-variation analysis, (c) double slab model for y-variation analysis, (d) model for x-variation analysis.

$$\phi^e(y) = A \cosh(n_3 y) \qquad 0<y<h \tag{83}$$

$$\phi^e(y) = B_c \cos[k_y(y-h)] + B_s \sin[k_y(y-h)] \qquad h<y<h+d \tag{84}$$

$$\phi^e(y) = C_c \cosh[n_1(y-h-d)] + C_s \sinh[n_1(y-h-d)] \qquad h+d<y<h+d+k \tag{85}$$

$$\phi^e(y) = D\, e^{-n_0(y-h-d-k)} \qquad y>h+d+k \tag{86}$$

where n_0, n_1, n_3 are attenuation constants in their respective regions and subject to a relation of equation (87).

$$k_z^2 = k_0^2 + n_0^2 = \varepsilon_3 k_0^2 + n_3^2 = \varepsilon_2 k_0^2 - k_y^2 = \varepsilon_1 k_0^2 + n_1^2 \tag{87}$$

where n_o must be real and positive, while n_1, n_3 may be either real or imaginary.

Matching the field components H_x and E_z at y=h, we obtain:

$$A \cosh(n_3 h) = B_c \tag{88}$$

$$\frac{A\, n_3 \sinh(n_3 h)}{\varepsilon_3} = \frac{B_s k_y}{\varepsilon_2} \tag{89}$$

and similarly at y=h+d

$$B_c \cos(k_y d) + B_s \sin(k_y d) = C_c \tag{90}$$

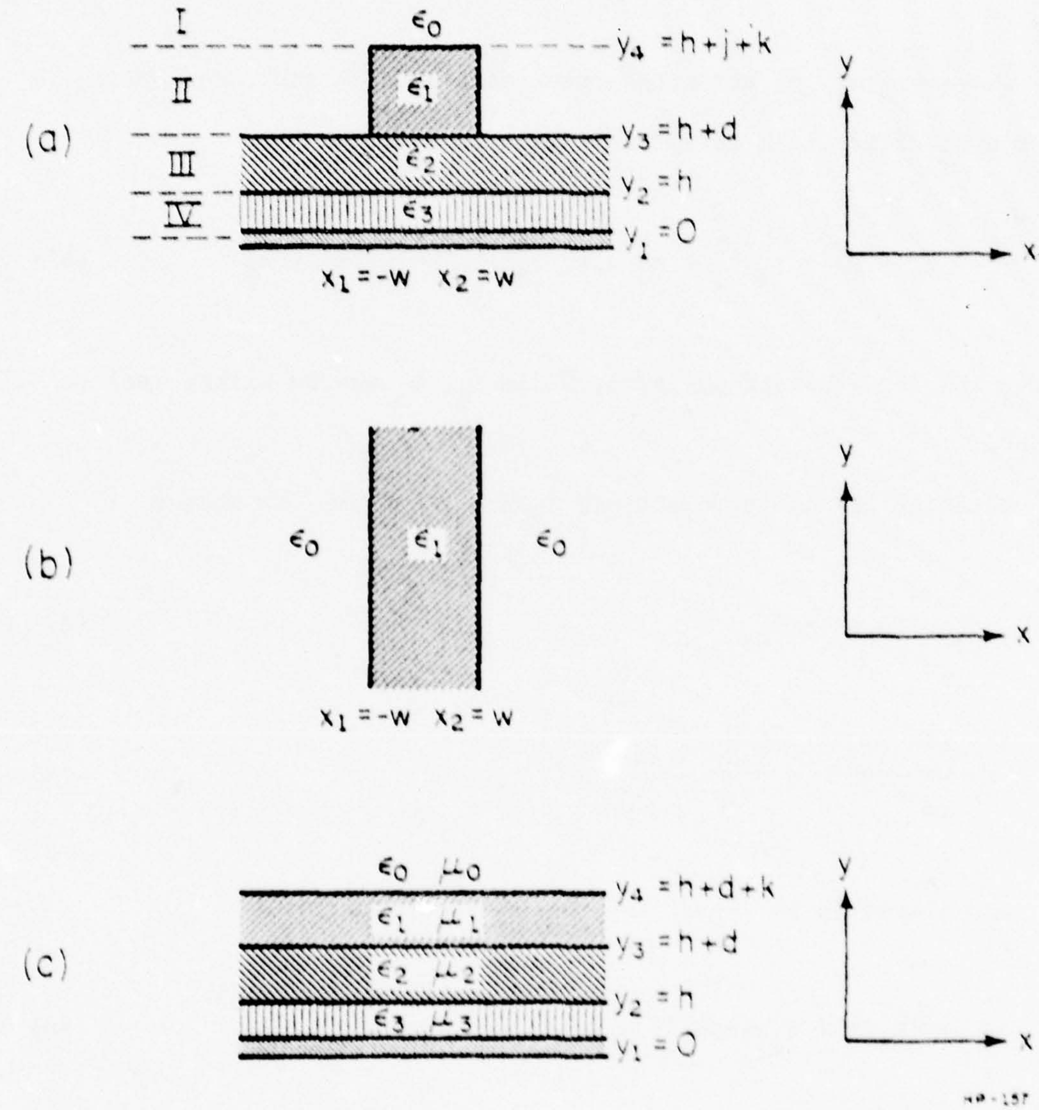

Figure 12. Analysis of strip loaded insulated guide by means of effective permeability method: (a) cross section, (b) model for x-variation analysis, (c) model for y-variation analysis.

$$\frac{-B_c k_y \sin(k_y d) + B_s k_y \cos(k_y d)}{\varepsilon_2} = \frac{c_s n_1}{\varepsilon_1} \tag{91}$$

similarly at $y = h+d+k$

$$C_c \cosh(n_1 k) + c_s \sinh(n_1 k) = D \tag{92}$$

$$\frac{n_1 C_c \sinh(n_1 k) + n_1 C_s \cosh(n_1 k)}{\varepsilon_1} = -n_0 D \tag{93}$$

After algebraically manipulating the six equations (88) through (93), we obtain:

$$B_c = A \cosh(n_3 h) \tag{94}$$

$$B_s = A \frac{n_3 \varepsilon_2}{k_y \varepsilon_3} \sinh(n_3 h) \tag{95}$$

$$C_c = A[\cosh(n_3 h) \cos(k_y d) + \frac{n_3 \varepsilon_2}{k_y \varepsilon_3} \sinh(n_3 h) \sin(k_y d)] \tag{96}$$

$$C_s = A \frac{k_y \varepsilon_1}{n_1 \varepsilon_2} [-\cosh(n_3 h) \sin(k_y d) + \frac{n_3 \varepsilon_2}{k_y \varepsilon_3} \sinh(n_3 h) \cos(k_y d)] \tag{97}$$

$$\begin{aligned} D = A[&\cosh(n_1 k) \cosh(n_3 h) \cos(k_y d) + \frac{n_3 \varepsilon_2}{k_y \varepsilon_3} \cosh(n_1 k) \\ &\sinh(n_3 h) \sin(k_y d) - \frac{k_y \varepsilon_1}{n_1 \varepsilon_2} \sinh(n_1 k) \cosh(n_3 h) \\ &\sin(k_y d) + \frac{n_3 \varepsilon_1}{n_1 \varepsilon_3} \sinh(n_1 k) \sinh(n_3 h) \cos(k_y d)] \end{aligned} \tag{98}$$

and the eigenvalue equation is:

$$\varepsilon_1 n_0 D + n_1 \sinh(n_1 k)\ C_c + n_1 \cosh(n_1 k)\ C_s = 0 \tag{99}$$

The effective dielectric constant ε_{eft} for this structure is:

$$\varepsilon_{eft} = \varepsilon_2 - \frac{k_y^2}{k_0^2} \tag{100}$$

After replacing regions I, III, and II by the hypothetical medium with the effective dielectric constants ε_{efd} and ε_{eft}, respectively, we may determine the propagation constant k_z by solving the problem as shown in Fig. 11(d). The procedure is the same as previously noted.

2) Effective Permeability Method: In Fig. 12(a), I have divided the strip-loaded insulated guide into four regions in the x-direction, and each of the regions is taken to be infinitely long in the y-direction. Regions I, III, IV are homogeneous regions, while region II is a single slab guide (Fig. 12(b)). From the analysis for inverted strip guide, we know that the eigenvalue equation is:

$$\tan\ (k_{x1} w) = \sqrt{(\varepsilon_1 - 1)\ k_0^2 - k_{x1}^2} / k_{x1} \tag{57}$$

The effective permeability for this structure is:

$$\mu_{ef1} = \mu_0 - \frac{k_{x1}^2}{\varepsilon_1 k_0^2} \tag{61}$$

We can now replace the single slab structure by a hypothetical $(\varepsilon_1, \mu_{ef1})$ region as shown in Fig. 12(c), and we may determine the propagation constant for this structure by equation (99) for triple-slab guide.

$$\varepsilon_1 n_0 D + n_1 \sinh(n_1 k)\, C_c + n_1 \cosh(n_1 k)\, C_s = 0 \tag{99}$$

and dispersion relation (101) is:

$$k_z^2 = k_0^2 + n_0^2 = \varepsilon_1\, \mu_{ef1}\, k_0^2 + n_1^2 = \varepsilon_2 k_o^2 - k_y^2 = \varepsilon_3 k_0^2 + n_3^2 \tag{101}$$

3) Iteration Method: We may use the same approach as previously noted: divide the guide structure into 12 regions and then use the effective ε method and the effective μ method to iterate.

G. Rectangular Guide

This structure has been analyzed by Klohn, Armata and Chrepta.[9] From their paper, this problem is solved by assuming the guide to be infinitely long in the x-direction and deriving the y-variation transcendental equation and, similarly, assuming the guide to be infinitely long in the

y-direction and deriving the x-variation transcendental equation. They treat each direction independently, and such a treatment is not reasonable. Their procedure can be modified by using effective ε and effective μ and getting more reasonable results.

1) Effective ε Method: The analysis is the same as described for the Inverted Strip Guide. First assume region II (Fig. 13(a)) is infinitely long in the x-direction, and get the ε_{ef1} for this region. After replacement, we obtain a structure as shown in Fig. 13(b). The propagation constant can then be determined by solving the eigenvalue equation for a slab-guide.

2) Effective μ Method: As shown in Fig. 13(c), region II is taken to be infinitely long in the y-direction. After matching the fields at the interfaces, we obtain μ_{ef1} for this structure.

After replacement, we arrive at a structure as shown in Fig. 13(d). The propagation constant can be easily determined for this structure.

3) Iteration Method: We can still use both the effective ε and the effective μ methods for iteration. The principal is the same as that summarized in E.

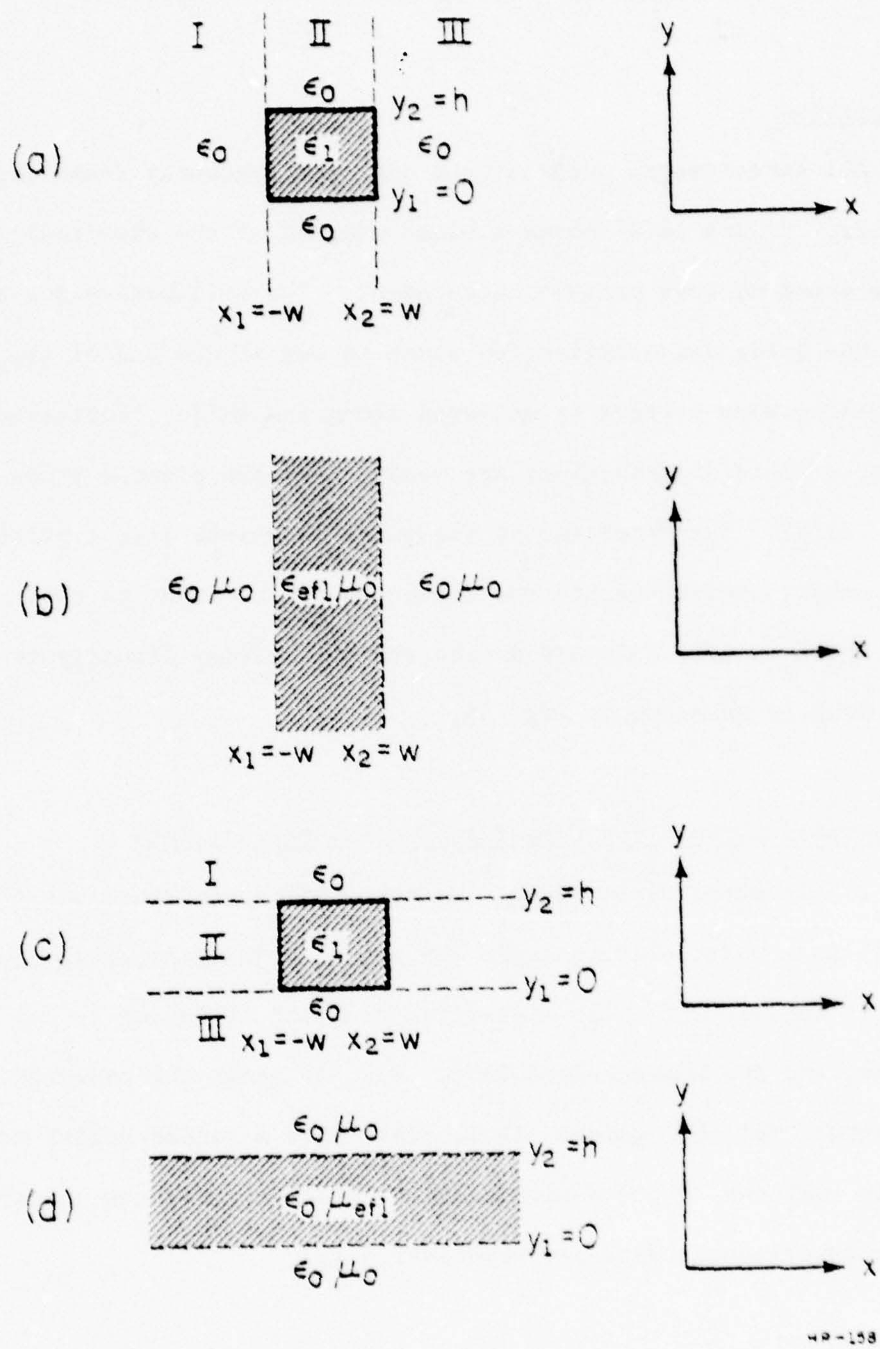

Figure 13. Analysis of rectangular guide
(a) Cross section for effective ε method.
(b) Model for x-variation analysis.
(c) Cross section for effective μ method.
(d) Model for y-variation analysis.

III. EXPERIMENTAL RESULTS AND NUMERICAL RESULTS

A. Apparatus

All experimental work is done over the frequency range from 78 GHz to 80 GHz. Figure 14(a) shows a block diagram of the experimental set-up for the standing wave pattern measurement. The millimeter-wave energy is fed to the guide and a reflecting plane is put at the end of the guide. The standing wave pattern is measured along the guide. Furthermore, the transverse field distributions are measured by the pinhole probe as shown in Fig. 14(b). The front end of the guide is shaped like a prism to enhance the launching efficiency and the direction of the input is chosen so as to excite the E^y_{pq} mode only and not to transmit energy directly to the problem. The feeding is as shown in Fig. 15.

B. Experimental Data and Comparison with Numerical Data

1) Inverted Strip Guide: We have made experiments for three cases. Case (a) is a Quartz-Teflon guide (QT guide). The dielectric constant of Quartz is 3.8, while the dielectric constant of Teflon is 2.1 h=1.61mm, and d=1.59mm and 2w=3.89mm. Fig. 16 shows the measured standing wave pattern for QT guide. It is clear that a second higher mode must exist in addition to the dominant mode. TABLE 1 shows the comparison between experimental data and numerical data:

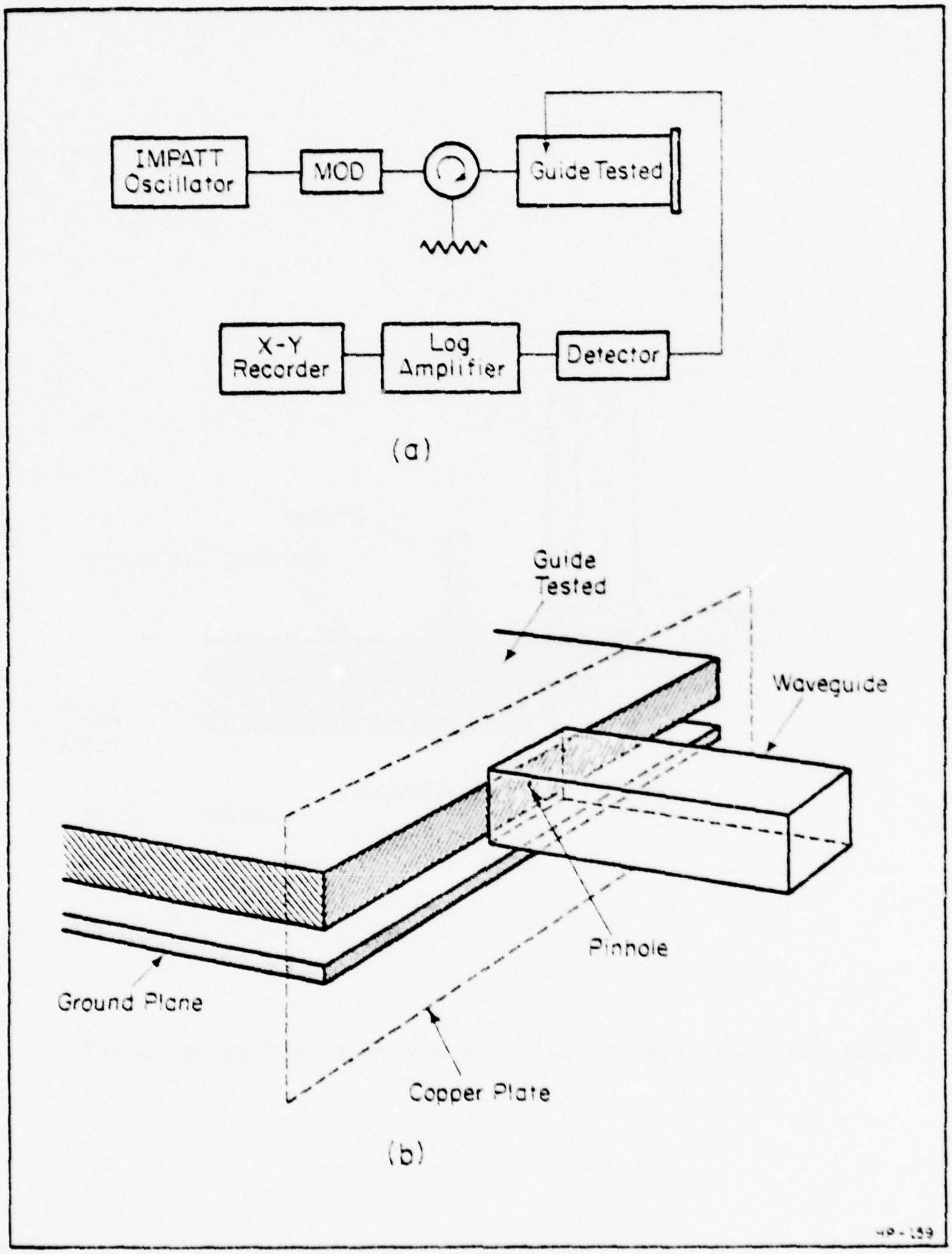

Figure 14. (a) Block diagram of experimental setup for standing wave pattern measurement.
(b) Pinhole probe.

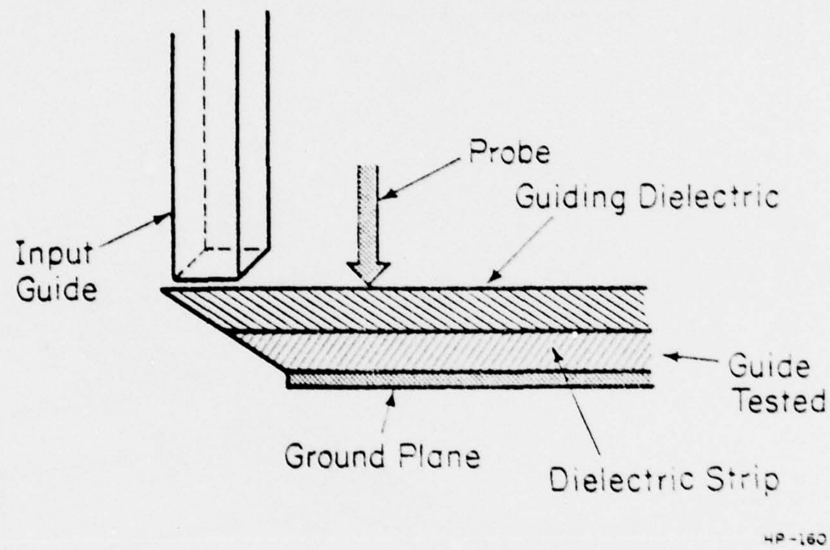

Figure 15. The prism coupling of energy to the guide tested.

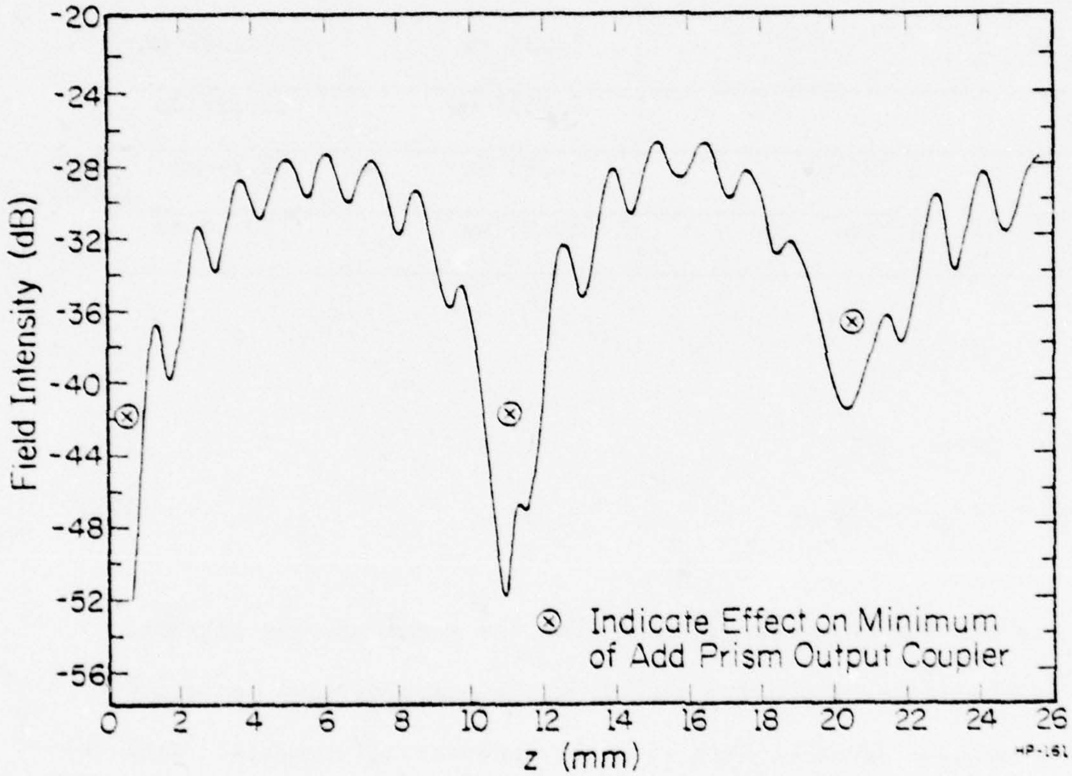

Figure 16. Standing wave pattern for QT guide.

TABLE 1

COMPARISON BETWEEN EXPERIMENTAL DATA
AND NUMERICAL DATA FOR QT GUIDE

f=79.4 GHz h=1.61mm d=1.59mm 2W-3.89mm

	Experimental Data	Effective ε Results	Effective μ Results
λ_1		2.232 mm	2.2/02 mm
λ_2		2.8035 mm	2.823 mm
λ_s	1.225 mm	1.243 mm	1.24 mm
λ_L	11 mm	10.95 mm	10.18 mm

where $1/\lambda_s = 1/\lambda_1 + 1/\lambda_2$ (102)

$1/\lambda_L = 1/\lambda_1 - 1/\lambda_2$ (103)

λ_s is the small wavelength seen from the standing wave pattern, while λ_L is the large wavelength seen from the standing wave pattern.

Both methods agree closely with the experimental results. Case (b) is a homogeneous inverted strip guide (HIS). The dielectric constant is 4.0, h=0.795 mm, d=0.735 mm, and 2W=2.05 mm. Fig. 17 shows the standing wave pattern for this HIS guide. There still exists a second higher mode. Table 2 shows the comparison between experimental data and numerical data.

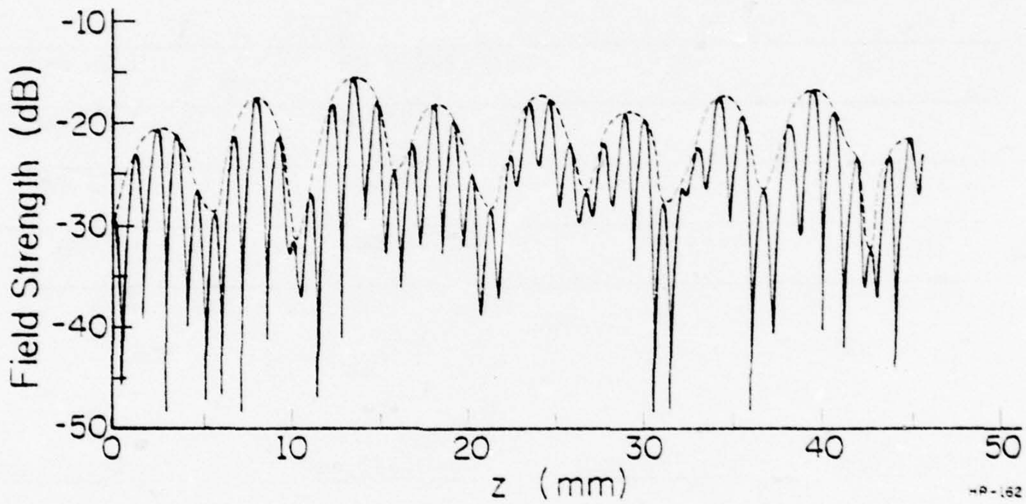

Figure 17. Standing wave pattern of guide HIS.

TABLE 2

COMPARISON BETWEEN EXPERIMENTAL DATA
AND NUMERICAL DATA FOR HIS GUIDE

f=79.4 GHz	h=0.795 mm	d=0.735 mm	2W=2.05 mm
	Experimental Data	Effective ϵ Results	Effective μ Results
λ_1		2.089 mm	2.08 mm
λ_2		2.507 mm	3.73 mm
λ_s	1.43 mm	1.14 mm	1.33 mm
λ_L	5.48 mm	12.51 mm	4.7 mm

f=78.7 GHz	h=0.795 mm	d=0.735 mm	2W=2.05 mm
	Experimental Data	Effective ϵ Results	Effective μ Results
λ_1		2.11 mm	2.10 mm
λ_2		2.54 mm	3.77 mm
λ_s	1.12 mm	1.15 mm	1.35 mm
λ_L	5.22 mm	12.52 mm	4.74 mm

where $\frac{1}{\lambda_s} = \frac{1}{\lambda_1} + \frac{1}{\lambda_2}$

$$\frac{1}{\lambda_L} = \frac{1}{\lambda_1} - \frac{1}{\lambda_2}$$

This time the effective ε method does not predict the 5 mm large wavelength, while the effective μ method does predict a large wavelength around 5 mm. Case (c) is a HIS guide again. (NHIS), the only change is the width, i.e., 2W = 1.0 mm. Fig. 18 shows the standing wave pattern for this guide. The pattern is very single-moded.

Table 3 shows the comparison between experimental data and numerical data.

TABLE 3

COMPARISON BETWEEN EXPERIMENTAL
DATA AND NUMERICAL DATA FOR NHIS GUIDE

f=78.8 GHz	h=0.795 mm	d=0.735 mm	2W=1.0 mm
	Experimental Data	Effective ε Results	Effective μ Results
λ		2.28 mm	2.28 mm
λ_s	1.26 mm	1.14 mm	1.14 mm

The results of both methods agree closely with the experimental data.

Figure 19 is the measured x-variation for the HIS guide. Fig. 20 is the measured x-variation for the NHIS guide.

2) Iteration Results: Table 4 is the iteration results for the Q.T. Guide at f=79.4 GHz. Table 5 is the iteration results for the HIS guide at f=79.4 GHz. Table 6 is the iteration results for the NHIS guide at f=78.7 GHz.

3) Strip-Loaded Insulated Guide: Fig. 21 is the standing wave pattern of this guide with a thin air gap. If we compare Fig. 21 with Fig. 17, it is clear that the former is much more single-moded than the latter.

Fig. 22 is the standing wave pattern of the NHIS guide with a thin air gap. It appears very single-moded.

Tables 7, 8, 9, and 10 show the comparison between experimental data and numerical data.

4) Rectangular Guide: Finally, the results of Klohn's[9] paper can be compared with the results obtained from the effective ε method, the effective μ method, and the iteration method.

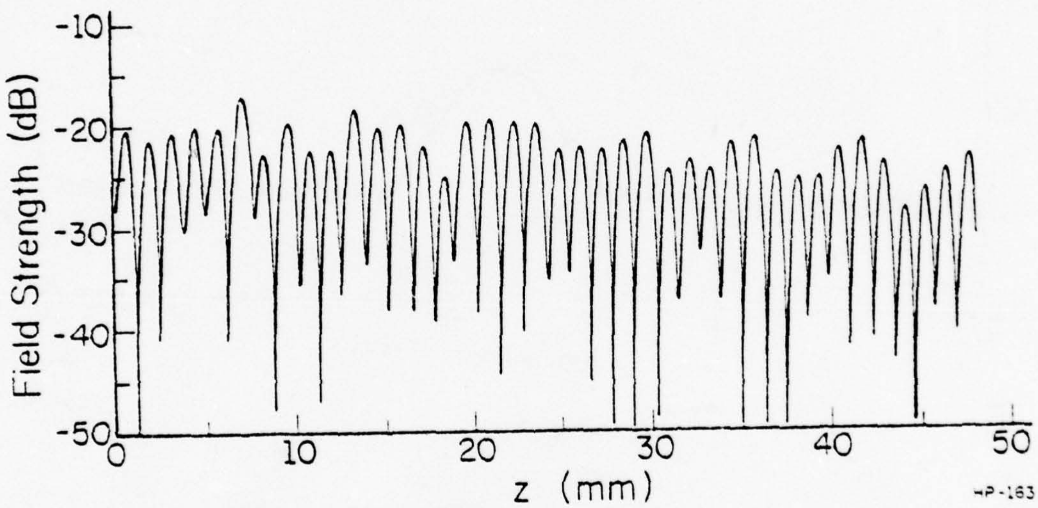

Figure 18. Standing wave pattern for NHIS guide.

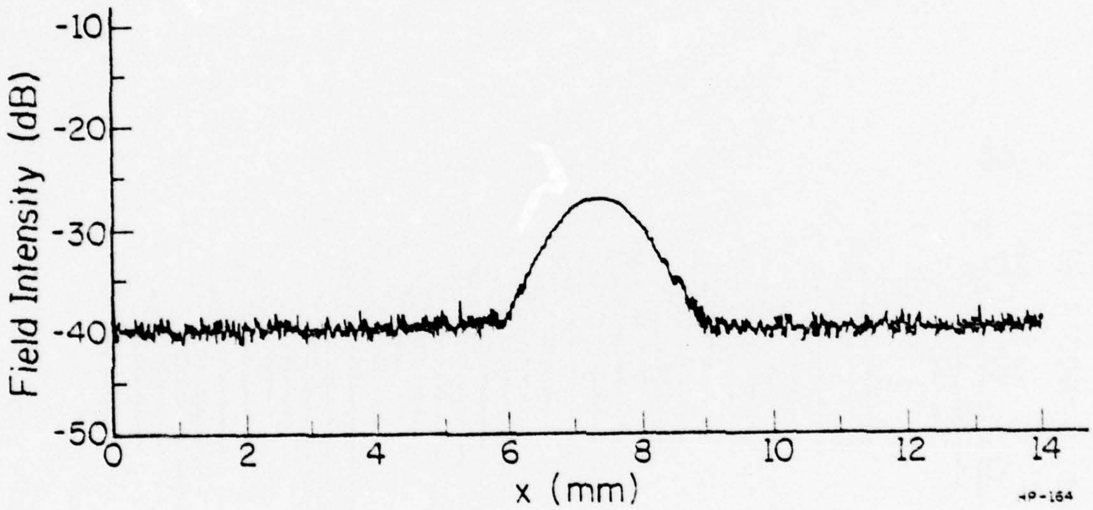

Figure 19. Field x-variation of HIS guide.

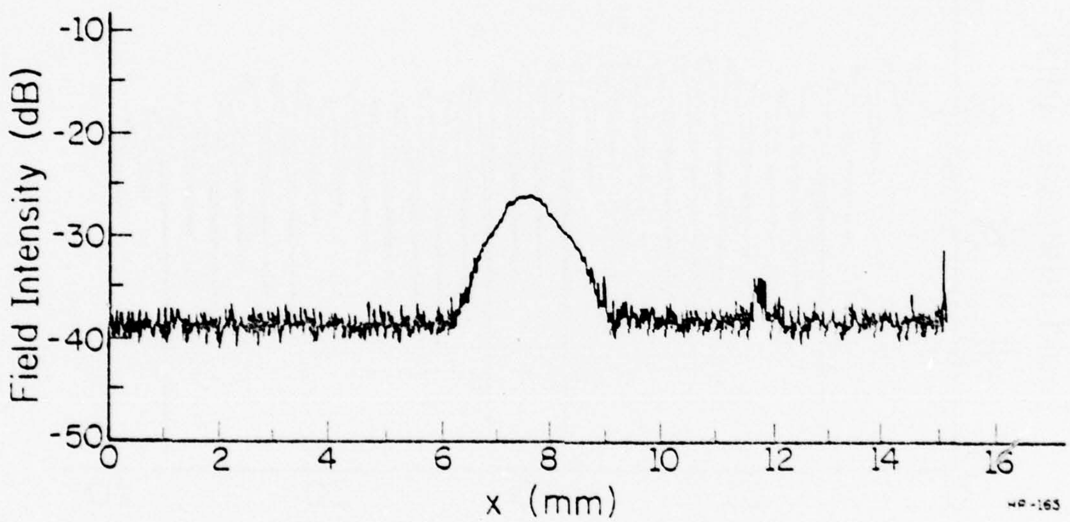

Figure 20. Field x-variation of WHIS guide.

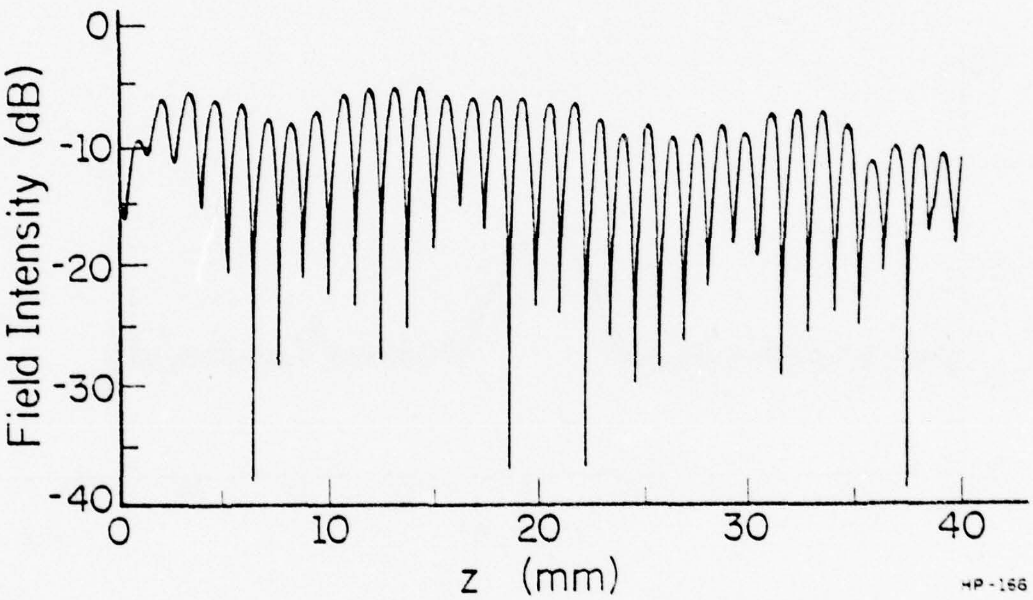

Figure 21. Standing wave pattern of insulated strip loaded guide (HIS guide with an air gap.)

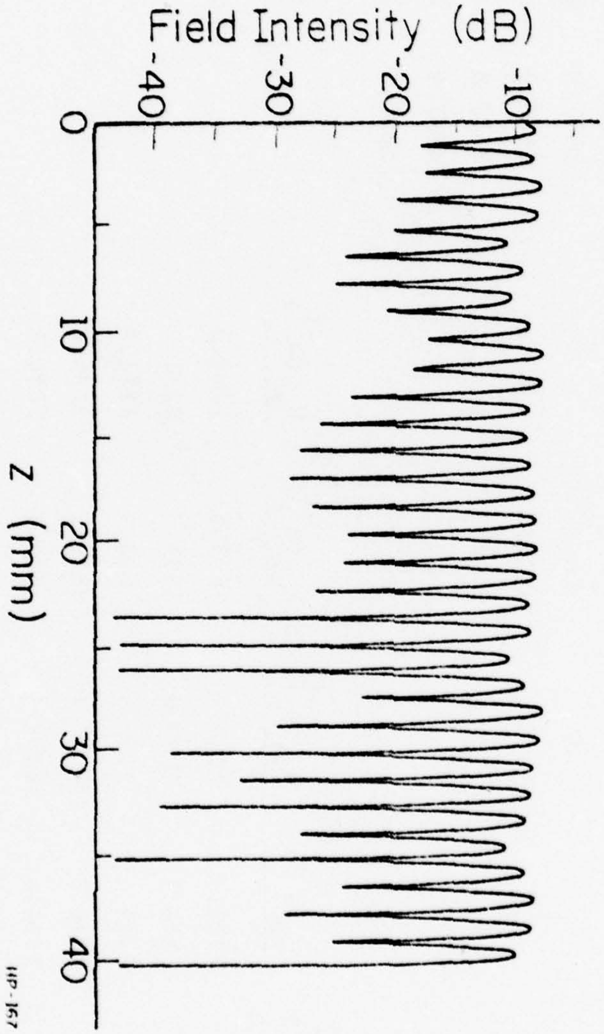

Figure 22. Standing wave pattern of insulated strip loaded guide (NHIS guide with an air gap).

TABLE 4(a)

QT GUIDE ITERATION RESULTS
EFFECTIVE ε METHOD, f=79.4 GHz

	$k_{x1}(m^{-1})$	$k_{x2}(m^{-1})$	$k_{x3}(m^{-1})$	$k_{x4}(m^{-1})$	$k_{x5}(m^{-1})$	$k_{x6}(m^{-1})$	---	$k_z(m^{-1})$	λ(mm)	λ_s(mm)
1		387.9			364.7			2834	2.217	1.1085
2		266.3			151.7			2837.2	2.214	1.1073
3		358.7			300.7			2837.9	2.214	1.107
4		358.7			300.7			2837.9	2.214	1.107
5		358.7			300.7			2837.9	2.214	1.107
6		358.7			300.7			2837.9	2.214	1.107
7		358.7			300.7			2837.9	2.214	1.107
8		358.7			300.7			2837.9	2.214	1.107
9		358.7			300.7			2837.9	2.214	1.107
10		358.7			300.7			2837.9	2.214	1.107

	$k_{y1}(m^{-1})$	$k_{y2}(m^{-1})$	$k_{y3}(m^{-1})$	$k_{y4}(m^{-1})$	$k_{y5}(m^{-1})$	$k_{y6}(m^{-1})$
1	1525.9	1542.5	2318.3	2263.9	1621.4	2263.9
2	1580.1	1550.3	2313.1	1969.0	1595.7	2282
3	1559.6	1547.4	2315	2125.8	1610.1	2271.9
4	1568.9	1548.7	2314.2	2047.8	1603.2	2276.8
5	1564.2	1548.1	2314.6	2087.1	1606.7	2274.3
6	1566.2	1548.4	2314.4	2067.5	1605	2275.5
7	1565.4	1548.2	2314.5	2077.3	1605.8	2274.9
8	1565.9	1548.2	2314.4	2072.4	1605.4	2275.2
9	1565.6	1548.3	2314.5	2074.9	1605.6	2275.0
10	1565.8	1548.3	2314.5	2073.6	1605.5	2275.1

TABLE 4(b)

QT GUIDE ITERATION RESULTS
EFFECTIVE μ METHOD, f=79.4 GHz

	$k_{1x}(m^{-1})$	$k_{x2}(m^{-1})$	$k_{x3}(m^{-1})$	$k_{x4}(m^{-1})$	$k_{x5}(m^{-1})$	$k_{x6}(m^{-1})$	$k_z(m^{-1})$	λ(mm)	λ_s(mm)
1	620.7	000.0	000.0	1631.2	000.0	000.0	2845.5	2.208	1.104
2	570.7	296.2	296.2	1150.0	192.4	192.4	2833.1	2.218	1.109
3	600.8	238.9	238.9	1412.5	119.8	119.8	2837.1	2.215	1.107
4	587.5	271.7	271.7	1287.5	158.6	158.6	2834.9	2.216	1.108
5	594.5	257.1	257.1	1351.5	140.5	140.5	2835.9	2.216	1.108
6	591.1	264.7	264.7	1319.9	149.8	149.8	2835.4	2.216	1.108
7	592.9	261.0	261.0	1335.8	145.2	145.2	2835.6	2.216	1.108
8	592.0	262.9	262.9	1327.9	147.5	147.5	2835.5	2.216	1.108
9	592.4	262.0	262.0	1331.8	146.4	146.4	2835.5	2.216	1.108
10	592.2	262.4	262.4	1329.9	146.9	146.9	2835.5	2.216	1.108

	$k_{y1}(m^{-1})$	$k_{y2}(m^{-1})$	$k_{y3}(m^{-1})$	$k_{y4}(m^{-1})$	$k_{y5}(m^{-1})$	$k_{y6}(m^{-1})$
1	1633.1	1557.5	2308.2			
2	1592.7	1552.0	2311.9			
3	1610.9	1554.6	2310.2			
4	1601.9	1553.3	2311.1			
5	1606.3	1553.9	2310.7			
6	1604.1	1553.6	2310.9			
7	1605.2	1553.8	2310.8			
8	1604.7	1553.7	2310.8			
9	1604.9	1553.7	2310.8			
10	1604.8	1553.7	2310.8			

TABLE 5(a)

HIS GUIDE ITERATION RESULTS
EFFECTIVE ε METHOD, f=79.4 GHz

	$k_{x1}(m^{-1})$	$k_{x2}(m^{-1})$	$k_{x3}(m^{-1})$	$k_{x4}(m^{-1})$	$k_{x5}(m^{-1})$	$k_{x6}(m^{-1})$	$k_z(m^{-1})$	λ (mm)	λ_s (mm)
1		1043.9			1907.0		3008.2	2.089	1.044
2		945.4			1376.6		2955.3	2.126	1.063
3		1006.4			1681.7		2996.1	2.097	1.049
4		984.2			1563.0		2989.3	2.103	1.052
5		998.3			1637.3		2992.1	2.100	1.050
6		991.6			1601.4		2990.1	2.101	1.051
7		995.0			1619.7		2991.2	2.101	1.050
8		993.5			1610.6		2990.7	2.101	1.050
9		994.2			1615.3		2990.9	2.101	1.050
10		993.8			1612.9		2990.8	2.101	1.050

	$k_{y1}(m^{-1})$	$k_{y2}(m^{-1})$	$k_{y3}(m^{-1})$	$k_{y4}(m^{-1})$	$k_{y5}(m^{-1})$	$k_{y6}(m^{-1})$
1	968.5	968.5	2714.7	1624.5	2380.9	1624.5
2	896.2	1203.9	2618.8	749.7	2058.7	2017.3
3	949.0	1042.8	2687.0	1187.4	2237.8	1816.5
4	935.7	1088.3	2669.0	951.4	2143.9	1926.5
5	943.5	1062.0	2679.5	1069.5	2192.1	1871.5
6	940.1	1073.6	2674.9	1010.1	2168.1	1899.2
7	941.9	1067.6	2677.3	1039.8	2180.2	1885.4
8	941.0	1070.5	2676.1	1024.9	2174.1	1892.3
9	941.4	1069.0	2676.7	1032.4	2177.2	1888.9
10	941.2	1069.8	2676.4	1028.6	2175.6	1890.6

TABLE 5(b)

HIS GUIDE ITERATIONS RESULTS
EFFECTIVE μ METHOD, f=79.4 GHz

	$k_{x1}(m^{-1})$	$k_{x2}(m^{-1})$	$k_{x3}(m^{-1})$	$k_{x4}(m^{-1})$	$k_{x5}(m^{-1})$	$k_{x6}(m^{-1})$	$k_z(m^{-1})$	λ (mm)	λ_s (mm)
1	1136.9	000.0	000.0	2648.6	0000,0	0000.0	3027.0	2.076	1.038
2	1098.6	912.7	912.7	2304.9	1237.9	1237.9	3001.4	2.093	1.047
3	1123.6	803.0	803.0	2522.4	865.8	865.8	3000.8	2.094	1.047
4	1113.5	874.4	874.4	2431.6	1093.4	1093.4	2999.4	2.095	1.047
5	1119.3	845.5	845.5	2482.9	995.5	995.5	2999.5	2.095	1.047
6	1116.6	861.2	861.2	2458.4	1047.4	1047.4	2999.4	2.095	1.047
7	1118.0	853.7	853.7	2471.0	1022.3	1022.3	2999.4	2.095	1.047
8	1117.3	857.5	857.5	2464.8	1035.1	1035.1	2999.4	2.095	1.047
9	1117.6	855.6	855.6	2467.9	1028.8	1028.8	2999.4	2.095	1.047
10	1117.5	856.6	856.6	2466.4	1031.9	1031.9	2999.4	2.095	1.047

	$k_{y1}(m^{-1})$	$k_{y2}(m^{-1})$	$k_{y3}(m^{-1})$	$k_{y4}(m^{-1})$	$k_{y5}(m^{-1})$	$k_{y6}(m^{-1})$
1	807.5	1394.5	2522.5			
2	928.4	1111.6	2659.3			
3	899.7	1194.7	2623.1			
4	916.7	1147.0	2644.2			
5	909.3	1168.2	2634.9			
6	913.2	1157.2	2639.8			
7	911.3	1162.6	2637.4			
8	912.3	1159.8	2633.6			
9	911.8	1161.2	2638.6			
10	912.0	1160.5	2638.3			

TABLE 6(a)

NHIS GUIDE ITERATION RESULTS
EFFECTIVE ε METHOD

	$k_{x1}(m^{-1})$	$k_{x2}(m^{-1})$	$k_{x3}(m^{-1})$	$k_{x4}(m^{-1})$	$k_{x5}(m^{-1})$	$k_{x6}(m^{-1})$	$k_z(m^{-1})$	λ (mm)	λ_s (mm)
1		1543.0			1500.6		2750.4	2.284	1.142
2		1273.7			942.1		2664.4	2.358	1.179
3		1438.7			1260.1		2713.4	2.316	1.158
4		1364.4			1108.4		2696.5	2.330	1.165
5		1398.7			1176.6		2708.9	2.319	1.160
6		1388.5			1156.0		2700.0	2.327	1.1635
7		1393.8			1166.6		2704.6	2.323	1.162
8		1391.2			1161.3		2702.4	2.325	1.1625
9		1392.5			1164.0		2703.5	2.324	1.162
10		1391.8			1162.7		2700.3	2.327	1.163

	$k_{y1}(m^{-1})$	$k_{y2}(m^{-1})$	$k_{y3}(m^{-1})$	$k_{y4}(m^{-1})$	$k_{y5}(m^{-1})$	$k_{y6}(m^{-1})$
1	968.0	968.0	2687.9	1594.5	2367.2	1599.5
2	756.1	1473.5	2447.6	1004.8	2161.2	1868.4
3	895.1	1204.1	2590.7	1279.0	2265.9	1740.0
4	843.8	1322.8	2532.2	1123.5	2208.3	1812.5
5	872.5	1260.1	2564.0	1198.1	2236.6	1777.5
6	859.3	1290.0	2549.1	1159.5	2222.1	1795.6
7	866.1	1274.7	2556.7	1178.5	2229.3	1786.7
8	863.0	1282.3	2553.0	1168.9	2225.6	1791.2
9	864.5	1278.5	2554.9	1173.7	2227.4	1789.0
10	863.6	1280.4	2553.9	1171.3	2226.5	1790.1

TABLE 6(b)

NHIS GUIDE ITERATION RESULTS
EFFECTIVE μ METHOD

	$k_{x1}(m^{-1})$	$k_{x2}(m^{-1})$	$k_{x3}(m^{-1})$	$k_{x4}(m^{-1})$	$k_{x5}(m^{-1})$	$k_{x6}(m^{-1})$	$k_z(m^{-1})$	λ (mm)	λ_s (mm
1	1788.6	.0	.0	2227.7	000.0	000.0	2756.9	2.279	1.1395
2	1685.4	1242.2	1242.2	890.4	888.9	888.9	2719.0	2.311	1.155
3	1745.2	985.1	985.1	2079.1	528.6	528.6	2719.5	2.310	1.155
4	1719.6	1141.9	1141.9	1996.6	733.5	733.5	2714.4	2.315	1.157
5	1733.7	1074.3	1074.3	2041.8	639.8	639.8	2715.3	2.314	1.157
6	1727.0	1110.4	1110.4	2020.2	688.7	688.7	2714.5	2.315	1.157
7	1730.4	1093.0	1093.0	2031.3	664.9	664.9	2714.8	2.314	1.157
8	1728.7	1101.8	1101.8	2025.8	676.9	676.9	2714.6	2.315	1.157
9	1729.6	1097.5	1097.5	2028.6	671.0	671.0	2714.7	2.315	1.157
10	1729.1	1099.7	1099.7	2027.2	674.0	674.0	2714.6	2.315	1.157

	$k_{y1}(m^{-1})$	$k_{y2}(m^{-1})$	$k_{y3}(m^{-1})$	$k_{y4}(m^{-1})$	$k_{y5}(m^{-1})$	$k_{y6}(m^{-1})$
1	288.0	1811.6	2209.0			
2	805.6	1395.1	2493.1			
3	664.1	1586.4	2376.0			
4	746.7	1486.8	2439.5			
5	709.9	1534.8	2409.6			
6	729.2	1510.4	2425.0			
7	719.8	1522.4	2417.4			
8	724.6	1516.4	2421.2			
9	722.2	1519.4	2419.4			
10	723.4	1517.9	2420.3			

TABLE 7

COMPARISON BETWEEN EXPERIMENTAL DATA AND NUMERICAL DATA FOR THE HIS GUIDE WITH A TEFLON INSULATION LAYER.

f=78.2 GHz	d=0.735 mm λ_s Experimental Data	k=0.795 mm λ_s Effective ε Results	2W=2.05 mm λ_s Effective μ Results
Case (a) h=1.593 mm	1.207 mm	1.157 mm	1.146 mm
Case (b) h=0.762 mm	1.161 mm	1.151 mm	1.134 mm
Case (c) h=0.256 mm	1.149 mm	1.116 mm	1.096 mm

TABLE 8

COMPARISON BETWEEN EXPERIMENTAL DATA AND NUMERICAL DATA FOR THE NHIS GUIDE WITH A TEFLON INSULATION LAYER

f=98.2 GHz	d=0.735 mm λ_s Experimental Data	k=0.795 mm λ_s Effective ε Results	2W=1.00 mm λ_s Effective μ Results
Case (a) h=1.593 mm	1.319 mm	1.215 mm	1.203 mm
Case (b) h=0.762 mm	1.242 mm	1.204 mm	1.183 mm

TABLE 9

COMPARISON BETWEEN EXPERIMENTAL DATA AND NUMERICAL DATA FOR THE HIS GUIDE WITH AN AIR-GAP INSULATION LAYER

f=78.2 GHz	d=0.735 mm λ_s Experimental Data	k=0.795 mm λ_s Effective ε Results	2W=2.05 mm λ_s Effective μ Results
Case (a) h=0.405 mm	1.196 mm	1.197 mm	1.188 mm
Case (b) h=0.7355 mm	1.218 mm	1.211 mm	1.202 mm
Case (c) h=1.066 mm	1.218 mm	1.213 mm	1.205 mm

TABLE 10

COMPARISON BETWEEN EXPERIMENTAL DATA AND NUMERICAL DATA FOR THE NHIS GUIDE WITH AN AIR-GAP INSULATION LAYER

f=78.2 GHz	d=0.735 mm λ_s Experimental Data	k=0.795 mm λ_s Effective ε Results	2W=1.00 mm λ_s Effective μ Results
Case (a) h=0.405 mm	1.265 mm	1.297 mm	1.291 mm
Case (b) h=0.7355 mm	1.299 mm	1.320 mm	1.323 mm
Case (c) h=1.066 mm	1.306 mm	1.328 mm	1.334 mm

TABLE 11

Case (a): 2W=1.58 cm, h=0.79 cm, f=16.4 GHz,

and ε_1=12

	k_{x2} (m^{-1})	k_{x3} (m^{-1})	k_{y1} (m^{-1})	k_{y2} (m^{-1})	λ_z (m)
Klohn's Calculated Results	178.9	1125.9	1071.2	390	5.66×10^{-3}
Effective ε Results	177.8	1060	1071.2	390	5.64×10^{-3}
Effective μ Results	178.9	1125.9	1056.2	389.9	5.66×10^{-3}
Iteration Results(ε)	178.4	1097.4	1070.1	390	5.64×10^{-3}
Iteration Results(μ)	178.6	1109.9	1069.1	390	5.66×10^{-3}
Experimental Results					5.8×10^{-3} m

TABLE 12

Case (b): 2W=1.55 cm, h=0.3 cm, f=16.4 GHz, and ε_1=12

	k_{x2} (m^{-1})	k_{x5} (m^{-1})	k_{y1} (m^{-1})	k_{y2} (m^{-1})	λ_z (m)
Kohn's Calculated Results	182.0	1125.4	613.7	960.7	9.25×10^{-3}
Effective ε Results	167.2	591.6	613.7	960.7	9.18×10^{-3}
Effective μ Results	182.0	1125.4	591	957.7	9.19×10^{-3}
Iteration Results (ε)	173.8	764.9	609.4	960.2	9.20×10^{-3}
Iteration Results (μ)	178.9	961.7	605.3	959.6	9.22×10^{-3}
Experimental Results					8.4×10^{-3}

TABLE 13

Case (c): 2W=0.5 cm, h=0.3 cm, f=16.4 GHz, and ε_1=12

	k_{x2} (m^{-1})	k_{x5} (m^{-1})	k_{y1} (m^{-1})	k_{y2} (m^{-1})	λ_z (m)
Kohn's Calculated Results	461.6	1042.4	613.7	960.7	1.184×10^{-2}
Effective ε Results	370.0	491.0	613.7	960.7	1.05×10^{-2}
Effective μ Results	461.6	1042.4	460.1	935.3	1.09×10^{-2}
Iteration Results (ε)	410.9	680.0	566.3	954.2	1.04×10^{-2}
Iteration Results (μ)	440.8	870.2	517.6	946.4	1.10×10^{-2}
Experimental Results					1.10×10^{-2}

IV. CONCLUSIONS

This paper presents a new approach to the analysis of millimeter waveguide, and it serves as a good check for the original effective ε method. Because both methods only give approximate results, a solution inspires more confidence if both methods agree.

A comparison of the results of both methods and the experimental data has been made, and the agreement has proven to be reassuring.

V. LIST OF REFERENCES

1. W. McLevige, T. Itoh, and R. Mittra, "New Waveguide Structures for Millimeter-Wave and Optical Integrated Circuits." IEEE Trans. Microwave Theory Tech., Vol. MTT-23, No. 10, October 1975.

2. Tatsuo Itoh, "Inverted Strip Dielectric Waveguide for Millimeter-Wave Integrated Circuits." IEEE Trans. Microwave Theory Tech., Vol. MTT-24, No. 11, November 1976.

3. R. M. Knox and P. P. Toulios, "A V-Band Receiver Using Image Line Integrated Circuits," Proc. of the National Electronics Conference, Chicago, Illinois, October 1974.

4. P. P. Toulios and R. M. Knox, "Image-Line Integrated Circuits for System Applications at Millimeter Wavelengths," U.S. Army Electronics Command, Final Report No. ECOM-73-0217-F, July 1974.

5. R. M. Knox, P. P. Toulios and J. Q. Howell, "Radiation Losses in Curved Dielectric Image Waveguides of Rectangular Cross Section," IEEE MTT-S International Microwave Symposium, Boulder, Colorado, June 1973.

6. P. P. Toulios, "Image Line Millimeter Integrated Circuits -- Directional Coupler Design," Proc. of The National Electronics Conference, Chicago, Illinois, December 1970.

7. P. P. Toulios and R. M. Knox, "Rectangular Dielectric Image Lines for Millimter-Wave Integrated Circuits," Western Electronic Show and Convention, Los Angeles, California, August 25-28, 1970.

8. R. M. Knox and P. P. Toulios, "Integrated Circuits for the Millimeter Through Optical Frequency Range," Proc. of the Symposium on Submillimeter Waves, Polytechnic Press of Polytechnic Institute of Brooklyn, April 1-2, 1970.

9. Kenneth L. Kloh, John F. Armata, Jr., and Metro M. Chrepta, "Transverse Propagation Constants in Dielectric Waveguides," U.S. Army Electronics Command, Research and Development Technical Report. Report ECOM-4242, August, 1974.

10. M. M. Chrepta and H. Jacobs, "Millimeter-wave Integrated Circuits," <u>Microwave Journal</u>, Vol. 17, November 1974.

11. M. M. Chrepta and H. Jacobs, "Millimeter-wave Integrated Circuits," 1974 IEEE S-MTT Int'l. Sumposium, June 1974.

12. Y. Chang and H. J. Kuno, "Millimeter-wave Integrated Circuits", Research and Development Technical Report, Report ECOM-74-0454-F in October 1975.

13. H. J. Kuno and Y. Chang, "Millimeter-wave Integrated Circuits," Final Report TR ECOM-73-0279-F, June 1974.

14. B. J. Levin and J. E. Kietzer, "Hybrid Millimeter-wave Integrated Circuits," U.S. Army Electronics Command, Final Report No. ECOM-74-0577-F, October 1975.

15. T. Takano and J. Hamasaki, "Propagation Modes of a Metal-Clad Dielectric-Slab Waveguide for Integrated Optics," IEEE J. Quartum Electronics, Vol. QE-8, February 1972.

16. T. H. Oxley, et. al., "Hybrid Microwave Integrated Circuits for Millimeter Wavelengths," IEEE MTT-S International Microwave Symposium, Chicago, Illinois, May 1972.

17. M. V. Schneider, "Millimeter-Wave Integrated Circuits," 1973 IEEE International Microwave Symposium, Boulder, Colorado, June 4-6, 1973.

18. E. A. J. Marcatilli, "Dielectric Rectangular Waveguide and Directional Coupler for Integrated Optics," BSTJ, Vol. 48, September 1969.

19. E. A. J. Marcatilli, "Bends in Optical Dielectric Guides," BSTJ, Vol. 50, March 1971.

20. R. F. Harrington, "Time-Harmonic Electromagnetic Fields," McGraw-Hill Book Company, Inc., New York, 1961.

21. "Special Issue on Millimeter Waves: Circuits, Components and Systems," IEEE Trans. on Microwave Theory and Tech., Vol. MTT-24, November 1976.

22. D. Marcus, "Integrated Optics," IEEE Press, 1973.

23. "Special Issue on Integrated Optics and Optical Waveguides," IEEE Trans. on Microwave Theory and Tech., Vol. MTT-23, January 1975.